*Manuscript
Click here to view linked References

Large range nanopositioning stage design: A three-layer and two-stage platform

M. Torralba[1*], M. Valenzuela[2], J.A. Yagüe-Fabra[3], J.A. Albajez[3], J.J. Aguilar[3]

[1]Centro Universitario de la Defensa, A.G.M. Carretera Huesca s/n, 50090 Zaragoza, Spain
[2]Departamento de Ingeniería Industrial, Universidad de Sonora, Rosales y Blvd. Luis Encinas s/n, 83000, Hermosillo, Mexico
[3]I3A, Universidad de Zaragoza, María de Luna 3, 50018 Zaragoza, Spain
*Corresponding author: Marta Torralba. Tel. +34 976 739 831. Fax +34 976 739 824. Email: martatg@unizar.es

Abstract

In this article, a novel two-dimensional nanopositioning platform (NanoPla) design is described. Its requirements are not only sub-micrometer accuracy for nanotechnology applications, but also long working range (XY-motion 50 mm x 50 mm). These features increase the common range operation of devices for nanotechnology issues (e.g. an atomic force microscope), and the number of potential metrological applications: positioning for manufacturing, manipulation or sample characterization. This novel design is characterized by a three-layer architecture and a two-stage motion strategy, which minimizes the measurement error. The manufactured prototype is here justified considering precision engineering principles and a wide state-of-art study of the literature, regarding long range nanopositioning stages. The simulations, the experimental results and the error budget also allowed, first, the optimization and, secondly, the validation of the design at nanometer scale.

Keywords: 2D-platform, Positioning, Long range, Nanotechnology, Atomic Force Microscopy

1. Introduction

Positioning stages act as supplementary units for measuring and manipulating samples at different working ranges. New systems and technologies have been developed to overtake the metrological challenges of accuracy, repeatability and stability when positioning is required at submicrometer or nanometer scale [1,2]. Nonetheless, a wide variety of applications demand not only these hard requirements, but also longer travel working ranges to increase the number of potential manufacturing and measuring tasks [3,4]. To obtain effective positioning, different options of metrological systems are currently available. Some of these systems are adequate for many demanding and accurate operations, but their measuring and positioning range is often very limited [5,6]. This is a drawback for tasks that require working with larger areas in a planar part (solar cells, foils, silicon wafers...), where cutting of specific samples may be necessary.

In order to perform precise and accurate movements along a wide working range, a two-dimensional nanopositioning platform stage (NanoPla) is presented in this paper. Its first application integrates an AFM as a suitable technique for micro- and nanometrology [7], due to the high vertical as well as lateral resolution in the topographic characterization task of specimens. The stage will increase the measuring range of that sort of instruments up to 50 mm x 50 mm, accomplishing nanometer resolution and submicrometer accuracy. A novel concept has been developed in a first prototype, which is characterized by its simpler design and compactness. The long motion range and the three-layer architecture are the main novelties of the design, which, together with a two-stage motion strategy, minimize the measurement error.

This article presents the main features and results after design, manufacturing and assembly of the platform. That includes an extensive review of state-of-art systems described in the literature, and used for similar applications, together with the application of many precision engineering principles in the design of the prototype. The design of the system has been optimized both by finite element simulation and by applying an error budget [8], in order to take into account the real performance of the components and their influence in the final positioning error. These techniques have allowed an important optimization of the design prior to its manufacturing.

2. Large range nanopositioning stage design overview

The importance of the performance features and the metrological challenge of miniature working conclude in different design principles and decisions, which characterize the operating aspects of large range nanopositioning stages. Thus, this work is based on precision engineering principles and a wide state-of-art study of stages found in the literature, to establish advantages and drawbacks of other machines applied solutions with similar applications. The aim is to propose an optimal design for the NanoPla system.

2.1. Nanopositioning stages classification

Nanopositioning stages could be classified into three different groups, considering working ranges and features, and the applied XY-stage structure (see Figure 1), being these three groups the following:

1. Ultra-high-precision CMMs: they may provide sub-nanometer resolution but with working ranges under 50 mm [9–12].
2. Stages with stacked linear axes: conventional designs based on stacked linear axes are characterized for long kinematic chains with an unfavorable force transfer behavior [13–16]. Generally speaking, stacking up driving systems limits the performance, on account of some additional drawbacks: large-size and unbalanced structure, lack of stability, accumulated geometric and assembly errors, necessity of sophisticated control systems, etc.
3. Plane stages: they present some advantages compared to stacked structures, considering precision design features. The co-planar scheme minimizes positioning deviations, so that it is applied in multiple systems [17–19], as well as in the here presented NanoPla stage.

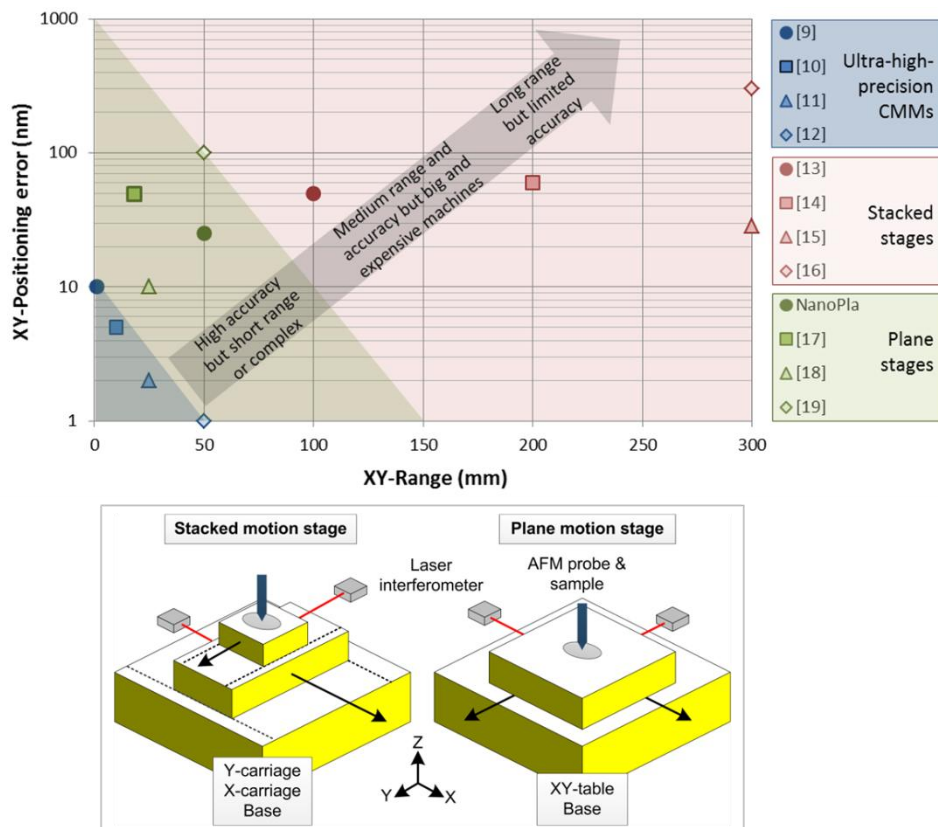

Figure 1. Nanopositioning stages classification scheme: XY-range vs. XY-positioning error (up) and stacked and plane motion stages: structural differences (down)

Structural differences between both conceptions are schematized in Figure 1. The stacked motion lodges one axis of displacement (Y-carriage) over the other one (X-carriage). The plane motion scheme locates an XY-table capable to provide displacements along two axes, which means different sensor arrangement and minimization of the measurement error. As well as this design decision, this work is focused on the comparison of different desirable features of found in similar system described in the literature. Thus, the aim is to develop, manufacture and assembly a long range nanopositioning stage justified in metrology issues.

2.2. Precision engineering principles: a summary

Different systems have been developed to cover applications that require the measurement of larger area substrates without previous preparation of small specific samples. Their design is based on precision engineering principles [20–22], which are summarized in Figure 2. They are related to the different systems, arrangements, materials and strategies applied, and become fundamental, if performance features are established at submicrometer scale. Hence, all of them suppose the basis of nanopositioning stage design.

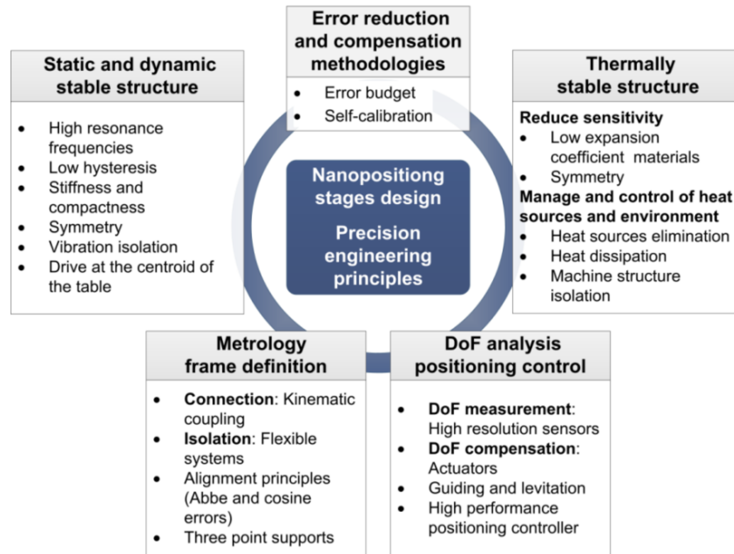

Figure 2. Summary of precision engineering principles for nanopositioning stages

2.3. State-of-art study of 2D-nanopositioning stages

Once presented the general design guidelines of precision engineering for 2D-long range stages, it is time to review different specific positioning prototypes found in the literature. The systems here analyzed are machines, platforms or stages with a minimum XY-travel range of approximately 5 mm (two-dimensional displacements, 2.5D or 3D) and intended for nanotechnology applications: SPM or Scanning Probe Microscopy (AFM in most cases), lithography, etc. Due to the significant number of developed systems and their similarities, each analyzed positioning stage is briefly presented in view of a design particularity that is considered relevant in this study. Then, all the presented stages are included in six main subsections: driving system, levitation system, metrology loop, motion stage structure, isolation and control strategy. This differentiation is also considered in the Table 1, where all the cited stages are summarized.

Table 1. Nanopositioning stages overview. Design features

2.3.1. Driving system

The critical decision of the actuator selection concerns the whole stage from the architecture to the control strategy and the possible guiding scheme. A summary of the diverse options for driving and guiding in nanopositioning is shown in Figure 3.

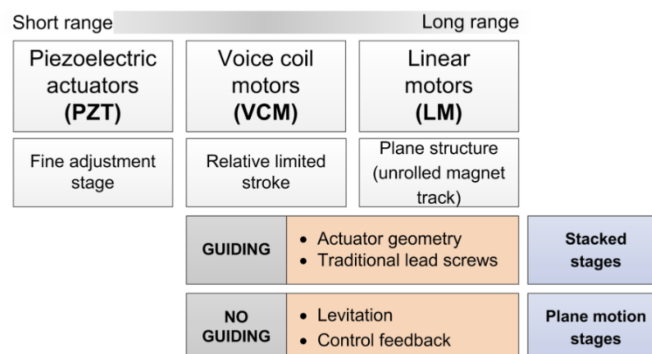

Figure 3. Drive and guiding system solutions

- **Piezoelectric actuators**

To carry out large travels, piezoelectric (PZT) solutions and flexure-based mechanisms are not adequate, in spite of the precise operation [23,24]. They serve as auxiliary units improving their performance of the large travel positioning stage, i.e. in the AFM scanning task. Two are the main options integrated in this kind of stages: voice coil motors (VCM) and linear motors (LM). Their direct coupling to the payload removes the problems of mechanical transmission elements such as lead screws, belts, rack-pinion and gear drives. Their configuration with no friction parts reduces the number of drive elements (simpler design) and increases the acceleration and speed (high dynamic characteristics and high servo bandwidth).

- **Voice coil motors**

Voice coil motors or Lorentz motors are a particular system that is nonexistent as a rotary option. Reversing polarity is used to change the motion direction avoiding commutation. That means no cogging, more simplicity and reliability. Other advantages of performance are their high bandwidth and easy control. The main drawback is the relative limited stroke and resolution [25]. Commercial solutions are available up to 100 mm approx., but with increased sizes in diameter and length, and poor performance. The Nano-Measuring Machine integrates these actuators [26]. Developed for heavy payloads and a medium long range of 20 mm x 20 mm, its XY-drive system is a stacked configuration of VCM and linear guides, which concludes in micrometer errors, not accurate enough for nanotechnology applications. Thus, VCM are inadequate by themselves for long ranges and high precision.

- **Linear motors**

Most used applied solutions are brushless DC motors. These linear motors are the combination of a coil and a permanent magnet assembly, with the peculiarity of the parallel and flat structure between both non-contact parts. They provide high forces and high speeds with a compact design. Less number of elements, no mechanical wear and simple maintenance are also advantages. Due to the absence of low-frequency resonances, linear motors increase the position loop bandwidth drastically, although they are more affected by disturbances. These actuators are also characterized by low stiffness, vibrations and velocity ripples, because of the control commutations. The precision along the motion is achieved by the integration of a guiding system and positioning feedback devices. Two are the configurations that lead the 1D-displacement: linear bearings and the own architecture of the actuator.

Linear bearings, such as traditional lead screws and linear rails, introduce the disadvantages of backlash, lack of stiffness, friction, vibrations, and maintenance. For this reason, some systems integrate an additional piezostage for fine adjustment to get accuracy. This is the case of the Dual-Axis Long-Traveling Nano-Positioning Stage [15]. For each axis in stacked configuration the system locates two lateral linear guides, one ball screw and one servo-motor to get high stiffness and speed. Air bearings are used to decrease friction forces.

In case of commercial available linear motors, the 1D-displacement is mostly leaded by the architecture of the magnet track: flat magnetic way, U-shaped (or channel) and tubular configuration. They impede the plane motion because of their design, even selecting broader magnetic arrays, so that they are commonly used in stacked nanopositioning stages. For example, the high large travel range platform presented by Yang et al. [16] obtains a macro-positioning system with high speed (up to 500 mm/s). Stacked configuration of the coarse XY-motion and the attached ultra-precision PZT positioning system achieve a combined positioning accuracy better than 3 μm, using U-shaped linear motors.

If the displacement along one axis is impeded due to the motor architecture, a planar motion is impossible to attain. As already said, the planar configuration can minimize geometrical errors, improve dynamics and stability and facilitate control tasks. For these reasons, home-made actuators are used to improve the performance of the stages. Based on ironless core to eliminate cogging, they achieve a more accurate and repeatable motion. One example of stage comprising home-made linear motors is the Multi-scale Alignment and Positioning System (MAPS) [11]. MAPS is an ultra-precision nanopositioning stage with 10 mm x 10 mm range. It incorporates different interchangeable

nanomanufacturing modules and characterization tools (e.g. AFM). MAPS excellent performance and the relevance concerning this work make the system our main reference nanopositioning stage.

2.3.2. Levitation system

To vertically sustain the weight of the moving platform and obtain a frictionless motion, a force in that direction should be created. Levitation is achieved by using air flows (air bearing stages) or by magnetic forces (maglev or magnetic levitation stages). In both cases, the absence of friction between mechanical parts as in traditional rolling bearings elements (e.g. balls or rollers) concludes with the benefits of infinite resolution, high accuracy, repeatability, speed, lack of wear, and no use of lubricants.

- **Magnetic levitation**

This kind of levitation is based on the creation of magnetic fields to generate opposite forces to the gravitational effect. One of the firsts developed maglev system was designed by Trumper and Kim [27], which decision is founded on accuracy issues and primarily set by sensors. Frame vibrations are attenuated by actively controlling transmissibility, and stiffness can be increased by servo control. Furthermore, fast responses and stability of the moving part of the stage depends on the difficult task of the control. Their wafer stepper was capable to provide large displacement in 2D (50 mm x 50 mm), with resolution better than 10 nm and high position stability. The single moving part simplifies the design and improves dynamics for photolithography applications. Posterior works of Kim finished in different long range maglev stages, such a novel platform with a plane motion over 5 mm x 5 mm area [28]. Its particular compact structure is the result of a special drive scheme. A Y-shaped platen integrates three actuators comprised of one moving permanent magnet and two coils located at different levels. Thus, vertical and horizontal forces can be created with continuous levitation control to balance the weight of the moving platform.

Another maglev stage has been developed by Holmes et al. [18] at the UNCC and MIT (Massachusetts Institute of Technology) collaboration: SAMM or Sub-Atomic Measuring Machine. With a position accuracy set in 10 nm, the special feature of the system falls on the suspension method. A lightweight platen is magnetically suspended and floating in oil, to reduce bias currents and provide viscous damping and high frequency coupling between the moving block and the machine structure.

- **Air bearing levitation**

Alternatively, nanopositioning stages can successfully integrate air bearings. An air flow through a porous surface of the bearing provides relative motion between the main stationary base and the positioning table. They are limited by airflows stability and bearing surfaces quality, which increases manufacturing costs. In addition, problems caused by friction between wires and pipes of the moving platform and stationary parts should be considered. High stiffness in vertical direction is achieved by the own weight of the moving part and diverse kinds of preload, as shown in Figure 4. The options are: (a) magnetic preload, (b) opposite air bearings arrangement, or (c) vacuum preload.

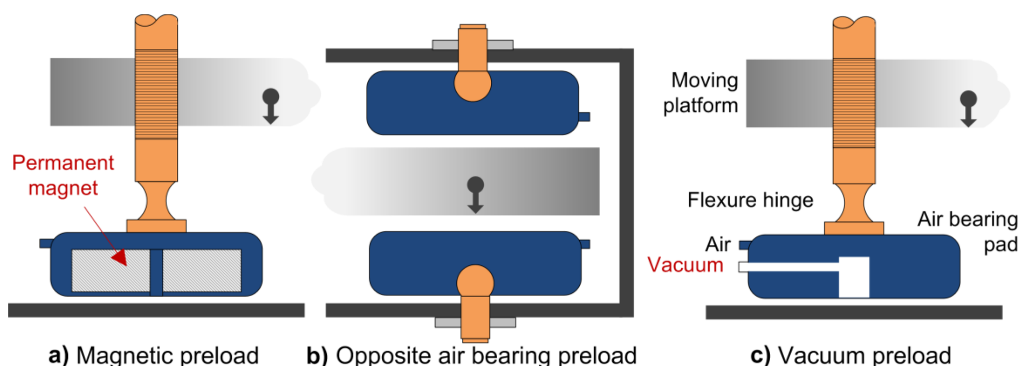

Figure 4. Air bearing preload solutions

Magnetic preload is applied in the planar motion stage of Dejima et al. [29]. Represented in Figure 4-a, the supporting unit includes a permanent magnet inside the air bearing pad. Thus, the magnet provides attraction force opposite to the levitation air flow. The stage can be controlled independently

in the five DoF (Degrees-of-Freedom) with 50 nm resolution. Another preloading option is the mounting of two opposed air bearings as in traditional CMMs for improving dynamic performance (Figure 4-b). In a first scheme, Chung et al. [19] designed a stage with four symmetric face to face pairs of air bearings, to compensate air flow pressure variations. However, the final used option was a magnetic preload, justifying the prototype in a detailed Finite Elements Analysis (FEA) [30]. Goal specifications of the system are a positioning accuracy of 1 μm and a minimum displacement resolution of 100 nm. Last option for air bearings preload consists in applying an additional attractive force in the center area of the element as a consequence of a vacuum air flow (Figure 4-c). An example of stage integrates these systems for levitation of the moving part is the result of Hesse et al. [17]. With a 100 mm circular travel range, three simultaneous linear drive units provide 2D-motions. Their flat coils are located in the structural base made of granite, just as the guiding surface of the air bearings (120º arrangement). The XY-servo error achieved is better than 1.3 nm.

2.3.3. Metrology loop

This subsection is focused on the metrology loop: sensors for the different DoFs and the metrology frame as a specific part of the whole system.

- **Sensors**

In order to obtain the actual position of the moving part, many sensors are available to be integrated in all the considered stages [31]. Measurement solutions with the aim of submicrometer accuracy can be classified according to several criteria. In this work, distinctions have been made between 2D- and 1D sensor systems, translation or rotation displacements and long and short range devices. Considering the 6-DoFs of a rigid body and summarized in Figure 5, possibilities to measure the long planar range of nanostages are (required DoFs): 2D-grid encoders and combinations of 1D-linear encoders and laser interferometers. Spurious motions in the out-of-plane positions (undesired DoFs) can be measured with the use of autocollimators (rotations) and capacitive or inductive sensors (short working range).

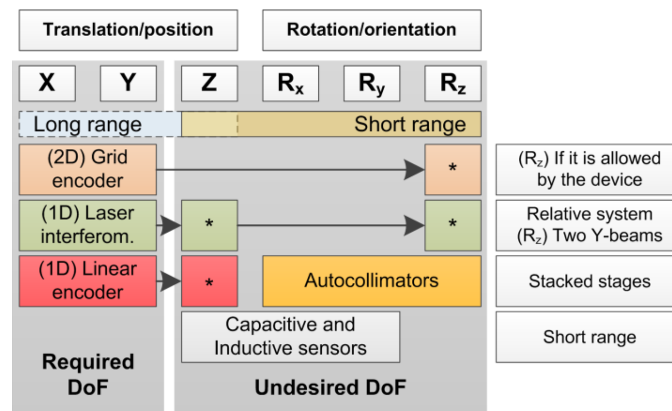

Figure 5. DoF and sensor solutions for nanopositioning stages

Positioning devices in a long XY-travel range are widely characterized by the use of 2D- and 1D-systems. In particular, two-dimensional grid encoders have a scanning head and a grid plate with a reference pattern on the surface. Thus, accuracy is a function of the quality pattern. For example, the air bearing stage presented by Ro and Park [32] integrates a commercial grid encoder to evaluate translations and rotation in the XY-plane. The moving plate locates the scanning head and the grid plate stays fixed. This sensor and the specific architecture of the machine conclude in compactness, but with the drawback of its 20 nm XY-resolution, especially high for some nanotechnology applications. Gao et al. presents a 40 mm x 40 mm planar stage with a home-made surface encoder [33]. The required 2D pattern plate was made with a particular grid of two-dimensional sinusoidal waves on its surface. To read them, two 2D-angle sensors were designed: first comprised by a quadrant photodiode and finally by a 2D-position sensitive detector to minimize linearity errors. The final integrated sensor is a 6-DoF surface encoder that composed of a planar scale grating and an optical sensor head [34]. This surface encoder could distinguish 2 nm step motions in the ΔX-, ΔY- and ΔZ-directions.

On the contrary, one-dimensional solutions commonly used for precision stages are linear encoders and, especially plane mirror laser interferometers (see Table 1). In this case, the obtained accuracy is not dependent on a 2D-reference grid.

Linear encoders, in their various configurations, can be integrated as the first option. They are more accurate than 2D-grid encoders. Manufacturing imperfections of linear scales are predictable and can be software compensated. However, due to their element parts (reading head and linear scale), they are not appropriate for plane designs. In addition, its traceability is ensured by an interferometry technique. As example, a prismatic 3D-CMM was developed by Vermeulen et al. [35] and lately commercialized by *Zeiss* under the name *F25* [36]. His singular architecture is similar to the prototype developed by Seggelen et al. [37]. It has a vertical slide probe attached to a moving platform whose displacement is measured by linear interference scales: incremental length measuring systems with glass-ceramic scales, providing 2.5 nm resolution and 250 nm accuracy (measuring range up 130 x 130 x 100 mm^3).

Other possible sensors for 1D-long range displacements are based on laser interferometry. Despite the relative high cost and wavelength variations as a consequence of the air refractive index changes, interferometry is the best option considering long range, accuracy and traceability issues. The here presented stage is the NMM-1 manufactured by *SIOS Meβtechnik*: Nanopositioning and Nanomeasuring Machine [1,38]. Their designed plane mirror interferometers stand out for the only one measuring beam, the stability of the He-Ne laser source and the fiber-coupled connection. This brings advantages to minimize Abbe error, to measure larger areas during several hours and to separate heat generation sources from the working area, respectively. In controlled environments, the closed-loop stability approx. 0.3 nm over the travel range of 25 mm x 25 mm x 5 mm.

Auxiliary sensor systems are required to measure and compensate deviations. Two are the desired DoFs in a plane motion stage: X- and Y-translations. Therefore, Z-stability and all rotations have to be characterized. For short displacements capacitive or inductive sensors are a common solution, in view of nanoscale requirements (sub-nanometer accuracy) and non-contact applications. Thus, out-of-plane parasite motions (tip, tilt and vertical errors) are evaluated in a short range. Other maglev stage PIMag® prototype of *Physik Instrumente*, and very similar to [17], is presented in [39,40]. The peculiarity of the system falls on the compact 6D-measuring head. For the XYR_z-DoFs the head integrates an optical sensor and a grid reference pattern in the slider or moving platform. For sensing tip-tilt motion as well as z-motion, capacitive sensors are arranged in pairs, using separated conductive surfaces: sensor heads and reference plates (1 nm resolution). Autocollimators are often used for rotational errors. In the stage presented by Eves in [41], three autocollimators are incorporated to determinate the orientation of the sample holder and correct the positioning with the action of six piezo-actuators. This system is accomplished by stacking two commercial stages (coarse and fine positioning) and attaches an AFM to increase up to 40 x 40 x 6 mm^3 the working volume.

- **Metrology frame**

The metrology frame is the part of the whole machine where the measurement takes place. Hence, its design is a key issue. Three are the aspects to take into account, besides material selection: connection by kinematic coupling, isolation by flexure systems and proper alignment to minimize geometric errors. The example here considered to study all the above characteristics is based on the design of Rujil [42], which performance characterization has been presented in different publications [43]. Commercialized by *IBS Precision Engineering* with the name of Isara 400 [44] is an ultra-precision CMM capable to integrate different probe systems with a 3D-measuring uncertainty of 109 nm (k=2) in the volume 400 mm x 400 mm x 100 mm.

First solved issue for the right metrology frame definition could be the material selection, important to avoid structural changes, because of thermal effects, force deformations and natural frequencies. To assure dimensional stability, low thermal expansion coefficient materials are fundamental. However, it is also important a high Young's modulus for stiffness and low density for lightweight structures. If internal heat sources exist, thermal conduction is also needed. Typically, metrology frames contains the sample and the sensors. Then, high structural solicitations are unusual. For these reasons, three are the most commonly used materials: Zerodur glass ceramic, Invar nickel-iron alloy and Silicon Carbide (SiC). In the Isara, Zerodur is used for the XY-moving reference platform that locates the

sample in a SiC table. Z-motion of the probe is defined by a second metrology frame: a vertical structure of SiC beams.

- Abbe error: Abbe's principle requires an alignment between the line of motion and the displacement measured. Isara stage measures all translations with plane mirror laser interferometers as positioning feedback. Three laser beams are pointed at the probe tip, and this alignment is constant during all motions over the entire volume. Therefore, Abbe principle is fulfilled in all axes, and straightness errors of installed linear guides and rotations do not have influence.
- Kinematic coupling: Three points of support are indispensable to connect parts and avoid instabilities. Additionally, a kinematic coupling has to be included, if the connection requires repeatable positioning [45]. Isara XY-moving platform rests in three flat air bearings, which are preloaded with the weight of the assembly. Over this, the SiC work piece table is sustained on three kinematic couplings to assure repeatability when mounting the diverse probes (quick and reproducible exchanges).
- Flexible coupling: When connection between elements involves decoupling, flexure systems [46] are needed. In the considered example, the join of the XY-drive system and the metrology frame was studied deeply to avoid deformation of the mirrors. This was accomplished with three air bearings and preload springs, not to transmit any forces in vertical direction.

2.3.4. Motion stage structure

To conclude, this subsection is focused on the motion stage architecture. It should be characterized by high stiffness and compactness (lower mass and avoiding stacking motion axes). Symmetry is also important to reduce errors, so that loads (as forces and heat) should be also symmetric for self-cancelling. Different configurations for achieving the 2D-displacements are here included. In addition, this point also considers the importance of materials and mechanical validation and optimization with specific Finite Element Analysis (FEA) software.

- **Global architecture**

In view of the actuators arrangement, the global architecture of a positioning stage can be different. The main distinction has been already done between plane and stacked stages (see Figure 1). The best option of planar configuration to obtain an accurate performance is only possible with actuators that provide 2D-motions. That means linear motors capable of attaining displacements along its drive axis (e.g. X-axis) and also along the orthogonal direction (Y-axis).

Despite of the suitability of plane structure options, several stacked stages have been developed with high accuracy requirements and excellent performance. It is worthy of note the system developed by Fan et al. [47,48]. Their micro-CMM (Coordinate Measuring Machine) was characterized for imitating the structure of conventional CMMs. It is made of Invar steel but with an arch-shape granite bridge for higher stiffness. Concerning XY-stage structure, its particularity is the co-planar design. To minimize Abbe error, the precision ground rods for both X- and Y-axis are located in the same plane, although stacked structure. Other structure similar to CMMs is the high precision profilometer of [49]. The structural frame is made of massive granite materials to support all the guiding systems in a stacked configuration. An applied architecture for stacked stages but extra-long ranges is an H-shaped frame as in [50,51]. The moving part is in the center of the system and the actuators are symmetrically placed on the sides. For this reason, performance in X- and Y-directions is not symmetrical. In particular, the stage presented in [50] incorporates a double H-structure: four linear motors (two for each X- and Y-axis) and respective guiding, to provide more rigidity, higher force and symmetry. One system with another specific design is the XY-coarse stacked stage of [14], which is attached in a cross architecture of perpendicular precision bars for horizontal guiding. A Zerodur plate acts as vertical reference surface to positioning a sample in a range of 200 mm x 200 mm. Flexure hinges and PZT actuators are used for fine adjustment (fine resolution about 1 nm).

To finish, a special 3D-configuration of the drive system is possible by the integration of a tripod configuration for three 1D- translation stages aligned with the center of the tip tool. For example, the lack of orthogonal motion axes as common stages implies in [52] a volume that is not a cuboid (20-40

cm^3). On the other hand, the Nanostage3D characterizes with the same architecture at nanometer scale samples in a 1 mm x 1 mm x 1 mm of travel range [9].

- **Materials and mechanical validation**

The XY-stage structure is not only a critical factor. The used materials and the FEA validation of the whole stage are also essential for the mechanical optimization (i.e. deformation and natural frequencies analysis). Considering individual parts and whole system, the material selection should conclude in a high stiffness and high Young's modulus, to provide a good static and dynamic behavior. According to this, and because of the necessity of lightweight moving elements, aluminum is one of the best solutions frequently used in a wide variety of nanostages. Its characteristics are numerous: low density, corrosion resistant, good heat conductor and easy and economic processing. Common alloys used, where aluminum is the predominant metal, are 6061 and 7075 (aircraft aluminum).

In view of the architecture validation, deformations and vibration modes are studied by Finite Elements Analysis (FEA) with the goals of (i) achieving the lightest moving platform and highest stiffness: Static analysis; and (ii) ensuring natural frequencies of the stage over the operation limit: Modal analysis. Different specific software is available to obtain numerical solutions of the above physical problems. Simulations are carried out during the design process, to conclude with the best geometry of main parts and couplings, and instruments distribution (e.g. in [30]).

2.3.5. Isolation

Regarding external influences, nanopositioning systems need to be as isolated as possible, to minimize the uncertainty of the final measurement result. Two are the main error sources at this point: vibrations and temperature changes. A representative example to analyze diverse isolation solutions is the Molecular Measuring Machine (M^3) [12]. Its architecture makes it different from all the stages with similar applications, due to the consecutive spherical layers that protect the machine core. Despite of the sophisticated design that provides subnanometer resolution, this scheme concludes in a very complex and big system

- **Vibration isolation**

Vibrations can be transmitted to the nanopositioning device through the support structure (environmental vibrations) and acoustically by the air (acoustic noise). Hence, it is necessary to set the machine on vibration isolation supports (active or passive tables), and even enclose it in a special covering. One of the protection layers of the M^3 is an active vibration isolation system to compensate possible mechanical resonances. Furthermore, the machine is supported by three pneumatic vibration isolation legs on a single concrete slab foundation.

- **Temperature isolation**

When it is possible, heat sources must be eliminated. Second option consists of dissipating the produced heat and last solution is the machine isolation. The spherical geometry of the M^3 maximizes stiffness and its symmetry provides thermal uniformity and stability. Related to the layers of the machine core, the first cover of the metrology frame is a temperature control shell. The environmental control strategy is based on maintaining the room at 17±0.01ºC and dispose thermocouples in the core, to achieve by heating a demonstrated temperature stability of 20±1 mºC. Likewise, material selection is founded also in thermal considerations, using Zerodur for the mirrored metrology box and Invar for linking components. An added vacuum chamber is also installed as an intermediate layer, to assure stability not only for the probe-sample interaction, but also for the laser wavelength.

2.3.6. Control strategy

The design of the control system in nanopositioning is a troublesome task by itself. This is the consequence of the elevated number of very heterogeneous hardware elements involved, combined with the high level specifications needed to achieve the established final accuracy. As already shown, it may be necessary for nanopositioning stages to combine different kinds of sensors and devices. Each has its own driver module and interface protocol to communicate with the main control unit (usually a PC), which might be a strong limitation for the sampling time used in the control loop. An equivalent problem also appears when the motion system is considered: very diverse actuators may

be combined in the same or different axis. To conclude, the final use of the platform introduces more elements to synchronize in the control: the implemented tool (for example, an AFM). Therefore, it would be really useful a methodology to support the integrated development of complex mechatronic devices. This could be the *Model-Based System Engineering* (MBSE) methodology [53] for the system-level design and the standard *System Modeling Language* (SysML) [54] as the tool to support the process [55]. Hence, to provide fast processing of signals and increasing the amount of treated data, powerful hardware and parallelization of data logging is decisive.

Concerning the control strategy, two different matters are in this part of the study considered: the motion system and the scanning type. First of all, the motion system affects because of the different control scheme: displacing the system (tool or sample) over the long range or using complementary coarse and fine stages. Secondly, the scanning type has also influence, because that considers how the tool is moving during the topographic characterization.

- **Motion system scheme**

The motion system strategy could differentiate between long ranges stages and systems with combined coarse and fine stages. If the driving motion is applied over the whole range with the demanded metrology requirements, e.g. AFM imaging is possible along several millimeters with the use of only one XY-stage. On the other hand, two different motions are carried out in the horizontal plane, regarding the sample or the probe: coarse approach and fine adjustments. In many cases, fine motion stages are used, in view of the impossibility to achieve submicrometer positioning in long travel ranges, although the control task becomes harder. When the scanning task is done with a separated fine stage, the whole range is characterized by the measurement of little areas. Consequently, a difficult treatment of images (e.g. stitching) turns a disadvantage of the combined motion system. Nevertheless, in both cases the scanning task is realized in a much faster and stable way, in a longer range and keeping a common reference for the entire measured area. That makes easier and more accurate images stitching when it is necessary.

An example for the first type is the system presented in [10]. This stage achieves the sample positioning in a long range for atomic force microscopy characterization. Due to the electronic microcontroller module, the motion resolution is around 10 nm. Once controlled the produced force by voice coil motors and using the sensor feedback, the root mean square value of position error is better than 5 nm.

When the 2D-long range stage cannot achieve the nanoscale requirements, systems integrate an extra positioning or fine adjustment motion. This is the sample-holder shown in [56]. Two independent approaches are considered. The coarse stacked stage provides the long range of motion with commercial linear motors. Piezoelectric actuators are on charge of the fine positioning. Its control strategy presents three scanning methods that sum up clearly the options with coarse and fine combination stages. "*Matrix by matrix*" mode scans the maximum motion area of the PZT-stage (3 μm x 3 μm). The main stage places the sample in all different matrices that compose the whole long range (50 mm x 50 mm). Stitching processes are needed due to the high accuracy in the home-made phase-shifting control developed for laser sensors. However, the problem is the time consumption. In order to obtain long and quick but not precise characterizations, "*line per line*" scans the sample with the coarse actuators along one direction and without fine adjustment. Finally, in "*tracking trajectory mode*" both actuators are enabled simultaneously. Fine stage compensates defects of the coarse positioning to ensure accuracy. The closed-loop control evaluates the deviation between ideal and real position. If the error is less than a limit at micrometer scale (accuracy of the long range stage), the control acts over short range motions, stopping coarse displacements.

- **Scanning type strategy**

Control is also affected by the scanning type of the used tool. The relative motion between the sample and the probe during the scanning task can be defined in three modes: scanning probe, scanning sample and separated tip and sample scanning. The first alternative moves the probe and keeps the specimen fixed. Hence, there are no limitations for sample sizes, weight or even shape (more flexibility), although Abbe error is unavoidable. On the contrary, the second option of fixing the probe and moving the sample is the best way to avoid the Abbe error in all the three axes, due to the stationary position of the measuring system. This is usual in commercial equipment. The third

alternative of combined motions involves diverse possibilities. Commonly separated XY- and Z-scanning motion improves dynamic behavior in vertical direction. A fast Z-motion is made by the probe, while the sample is moved over the horizontal plane.

The vacuum compatible system of Buice et al. moves the specimen onto the moving platform, while the tool keeps stationary [57]. That provides an easy interchange of a variety of probes (i.e. pick and place manipulators, scanning microscopes…). As the tool is fixed, control task is focused on the positioning sample stages, here achieved with a multi-DoF cascade (stacked coarse and fine configuration). Second configuration appears in the commercial Ultrahigh-Accurate 3D-Profilometer or UA3P [13]. The system keeps constant the atomic force generated between the AFM tip and the sample, regarding motions of the scanning probe. Hence, the tool is connected to an XYZ-stage. Different scanning types are programmed for spherical lenses characterization, to assure high accuracy in long diameters. When the positioning of the sample or probe is not achieved in all three XYZ-axis, a combined scanning is required: e.g. controlling the sample motion in XY-plane and providing vertical displacements from the tool module. This is the case of the Sawano et al. system [58]. The presented CMM is based on a planar nano-motion stage and a vertical system. The XY-table is driven by eight VCMs and the Z-stage integrates VCMs and PZTs as actuators for coarse and fine motions, respectively. Combined control differentiates between the XYR_z-closed loop (PID and acceleration feedforward compensator) and Z-compensators (coarse and fine motions keeping constant tunneling current between the probe and specimen surface). In a similar XY-positioning stage, force estimation is used for nano-machining control task in [59].

3. NanoPla final design

Once presented the wide review study of design requirements and used solutions for nanopositioning stages, this section summarizes the characteristics of the developed prototype. The goal pursued with the NanoPla design has been to overcome the main weak points detected in former designs of nanopositioning systems in order to obtain a design with planar movement, being also compact and modular. Hence, the main design characteristic of the NanoPla stage is the novel arrangement based on compactness for a long travel range in nanopositioning applications. This is achieved thanks to the novel three-layer solution shown in Figure 6, comprising a fixed superior base, a moving central platform and a fixed inferior base. The final size of the whole machine is approximately 600 mm × 600 mm in the footprint, and approximately 200 mm in height. This design assures the characterization of big samples, thanks to a motion capability up to 50 mm × 50 mm.

In the following sections and subsections the different components used, the precision engineering principles applied and the design methodology followed are exposed in order to justify the suitability of the design.

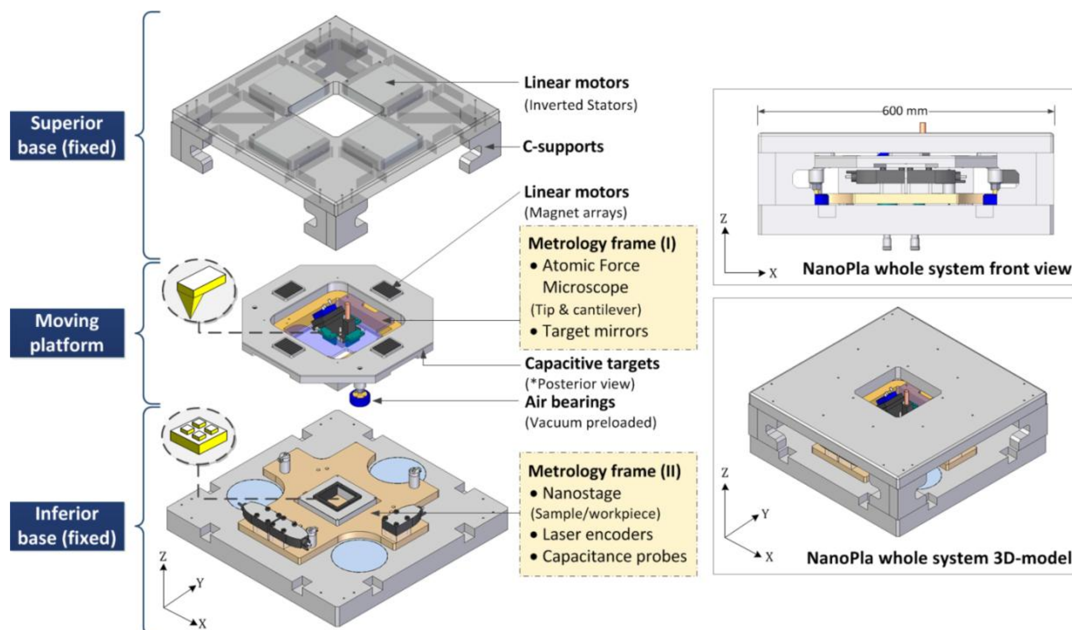

Figure 6. Three-layer NanoPla architecture

3.1. Superior base

The superior base of the NanoPla stage is characterized by the driving system. Since the system provides plane motion, linear motors have been used as long range actuators, instead of VCMs and PZTs with limited displacements. The Halbach home-made actuators used were defined considering the NanoPla XY-long travel range: 50 mm x 50 mm, besides the required forces to displace the moving platform. The size in the winding effective area allows the interaction between the stator and magnet array in all positions along the plane moving range, i.e. the stator is wide enough to cope with the lateral movement of the magnet array. Their original design was made by Trumper et al. [60], and they have been integrated in different high-precision nanopositioning stages. Hence, their performance has been demonstrated in multiple previous works, such as in maglev stages [27,28], and in the UNCC projects MAPS and SAMM [11,18].

The NanoPla linear motors were manufactured at the Center for Precision Metrology at the UNCC and are capable of creating dual forces (F_x and F_z), which is schematized in Figure 7. NanoPla linear motors are composed by a Halbach array of eight magnets bounded into aluminum housing that concentrates the magnetic flux on one side of the magnetic way. DC currents are sent through each stator phase of the coil winding. The three phases of winding are wrapped around an anodized aluminum mandrel. Two reasons make aluminum the best option: absence of iron minimizes cogging and high thermal conductivity attains to dissipate the generated heat by the coils away from the work area. The tests accomplished confirm the performance of these forces according to their theoretical behavior [61]. That means the sinusoidal force profile for each motor phase is a function of the electromagnetically interaction between both parts and the magnet array position in relation to the stator.

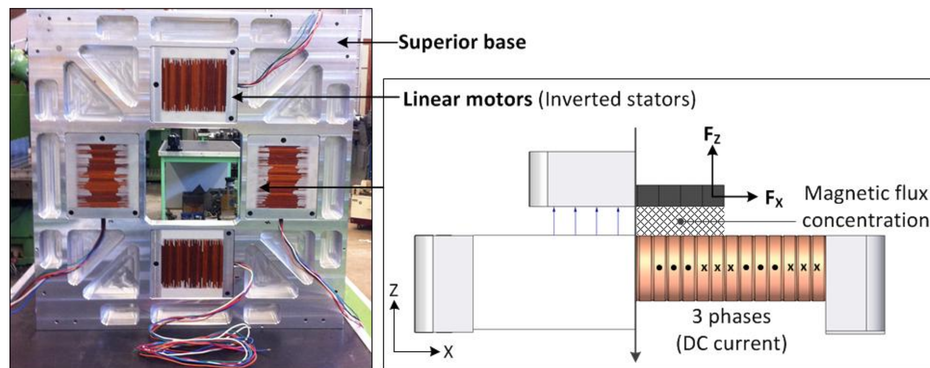

Figure 7. Superior base assembly (left) and the linear motor scheme (right)

This superior base, made of aluminum, lodges the four stators (2 along X and 2 along Y) in an inverted position (see Figure 7), facing down the magnet array, that are placed on the central moving platform. Apart from that, the access to the AFM and the samples is carried out through the central aperture of this base. The goal of this scheme is to reduce the size of the stage, as an advantageous solution for improving metrological performance. The drawback is supporting the weight of these stators. Nevertheless, stiffness can be achieved with a rigorous mechanical design (FEA analysis). The superior base stands on eight C-shaped supports. Additionally, the location of the stators on the top of the system, on the outline of the platform and embedded on the aluminum of the base minimizes the possible thermal affection of the motors to the accuracy of the system. The heat generated is easily dissipated with minimum affection to the central part of the stage, where the metrology frames are located.

3.2. Inferior base

The inferior base, together with the superior base, provides the structural stiffness. This part accomplishes three main functions: 1. It acts as the base for the levitation system of the central moving platform; 2. It contains the metrology frame, where the static part of the different measuring systems used are placed; and 3. Attached to this metrology frame, a nanopositioning stage with a sample holder provides the motion for the scanning of such sample.

3.2.1 Structural frame

The structural frame of the inferior base is made of aluminum. That supports the fixed metrology frame and incorporates a central hole to provide accessibility and devices handling. This part also lodges the three flat surfaces that act as the references for the air bearings that levitate the moving platform (see Figure 8). To check the adequate operation of the air bearings, the flatness and parallelism of the reference surfaces was measured. These circular reference surfaces were made of F114 steel, with a flatness tolerance of 3 μm and a thickness of the plate of 15 mm. The surface finish processes used were hard chrome plating, posterior finished by linishing. Each plate is screwed to the base with a single central bolt that allows the adjustment of the screwing force and, therefore, of the flatness of the reference plates. As can be seen in Figure 8, an excessive force could bend the surface. During the assembly of the stage, these parameters have been experimentally characterized with a CMM (see Figure 8).

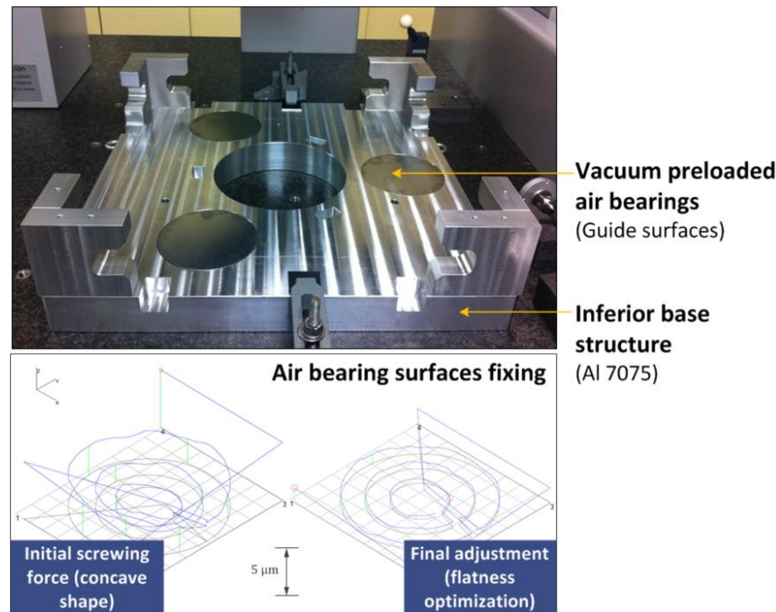

Figure 8. Inferior base assembly and air bearings surfaces adjustment

3.2.2 Fixed metrology frame

The metrology frame installed in the inferior based kept fixed during operation, in view of the main reference system of the stage. The final material of this part will be Zerodur® to assure negligible dimensional changes when temperature changes, due to its low thermal expansion coefficient. However, in this first prototype aluminum was used instead for preliminary tests of the first prototype. Even though, the metrology frame has been connected to the structural frame through three flexures, in order to cope with possible deformations as it will be in the final design. Thus, the entire frame is connected by three identically spaced flexure mounts (three supports connection) to diminish thermal gradient effects. Kinematic couplings are not still evaluated, due to the fixed positioning of all elements in the prototype. Symmetric design is also considered.

This block is mainly formed by the piezostage, sensor arrangement and the metrology frame structure (see Figure 9). Since both required and undesired translations and rotations want to be determined, all the six Degrees-of-Freedom are measured by high resolution sensors. Regarding the sensor system, their static parts have been located on this base. For the long range and plane motion, plane mirror laser interferometers are the best solution. Their justification is based on the high accuracy level reached and its direct traceability, despite their cost (accuracy of grid encoders depends on the grid quality). The measurement of the spurious motions is accomplished by the short-range devices: capacitance probes.

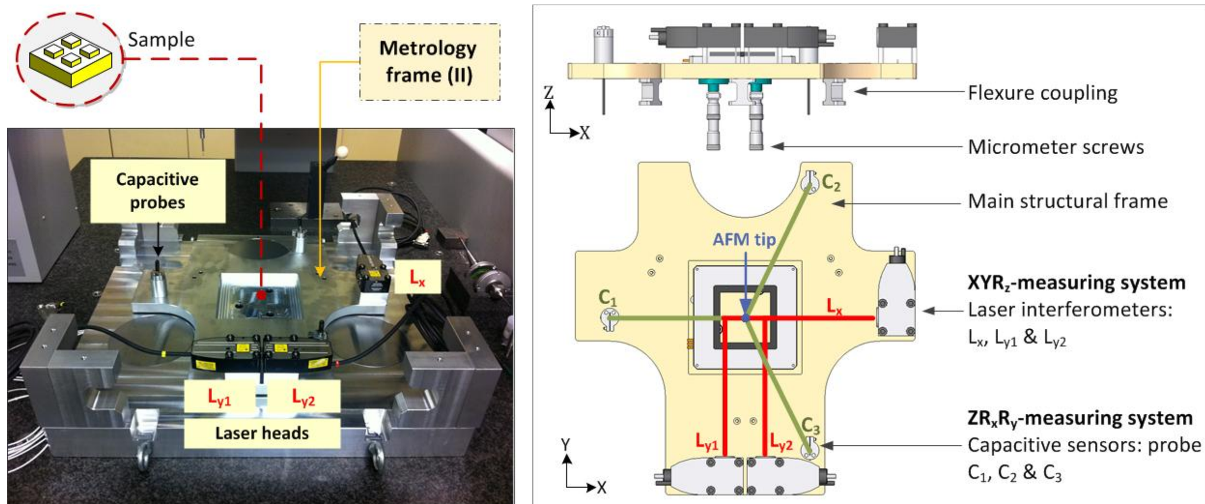

Figure 9. NanoPla metrology frame (II): components

First of all, three plane mirror laser interferometers to measure the long range displacements of the moving platform along X (1 laser beam) and Y (2 laser beams), as well as the rotation around Z. Then, one laser head is placed in the X-axis (L_x lecture), aligned with the reference system of the travel range. Two parallel laser beams are located in Y-axis (L_{y1} and L_{y2} lectures), symmetrically to the orthogonal axis of the reference system. The plane mirror laser interferometers provide a resolution of 2 nm (after interpolation). The sensors selected are the Renishaw RLU laser units and REE interpolators, connected to three RLD10 detector heads and three RCU10 environmental units for compensation the influence on the laser wavelength of the refractive index variations. Two plane mirrors made of Zerodur act as reflectors installed in the moving platform.

In addition, three capacitive sensors placed vertically to measure the spurious motions: rotations around X and Y and displacement along Z. The three probes are approximately equally spaced. The capacitive sensors used were the Lion Precision C5-E, with a sensing area of Ø0.8 mm, a whole range of 100 µm and 10 nm as standard resolution, which entails easy assembly, compactness and high precision performance. The Driver selected was the Elite Series CPL190 Driver.

Regarding the Abbe error, it has been minimized by design. An adequate alignment between the laser beams and the AFM tip was obtained by design, making the AFM tip coincident with the center of the reference system formed by the three lasers, as shown in Figure 9. Hence, deviations for XY-motions are minimized. First and second order errors will depend on the assembly and the precise performance of the nanopositioning stage that moves the sample during scanning. Nevertheless, the AFM and nanostage control act for keeping constant the cantilever deflection. If the tip is almost fixed during the surface measurement, this geometric error should be negligible.

3.2.3 Nanopositioning stage

Due to the demanding requirements of nanometer resolution, stability and sub-micrometer accuracy, a two-stage scheme has been applied in this prototype. It means the combination of the XY-long range moving platform here presented and an additional fine nanopositioning system for the scanning operation. This second stage is characterized by a piezoelectric drive. In brief, the moving platform moves the AFM accurately to different areas of big substrates, while the auxiliary nanopositioning unit provides the sample with the motion needed for the scanning (see Figure 10). With this two-stage strategy, the scanning task is carried out not only in a much faster and stable way, but also in longer ranges (50 mm x 50 mm), keeping a common reference for the entire measured area. The stage selected was the nPoint NPXY100Z10A, with a moving range of 100 µm x 100 µm x 10 µm. The C-300 series unit of the same company is in charge of the closed-loop control.

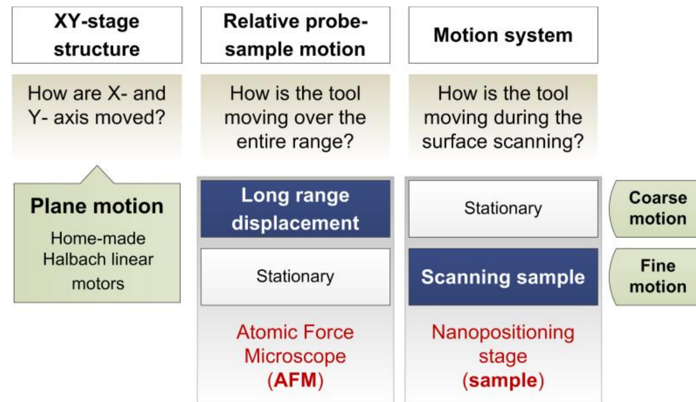

Figure 10. NanoPla control strategy scheme. Summary

As shown in Figure 10, the commercial nanopositioning stage for the scanning sample is positioned in the center of the metrology frame. It will be supported by a kinematic coupling over a micrometer screw with spherical tip (necessarily preloaded). These micrometers provides to the stage vertical displacement, and tip and tilt adjustment. By motorization of one of them, they also serve as a part of the control loop for approaching sample and AFM tip.

3.3. Moving platform

The moving platform is the part of the stage to be moved and accurately positioned by the system along the large range of 50 mm x 50 mm. It is mainly formed by two frames connected by three flexures: 1. Structural frame; and 2. Metrology frame (I).

3.3.1. Structural frame

The structural frame of the moving platform is presented in Figure 11. It lodges the moving part of the linear motors previously described (i.e. the magnet arrays). Then, as in the other parts, aluminum alloy 7075-T6 has defined as its material, which means lightness and good mechanical properties.

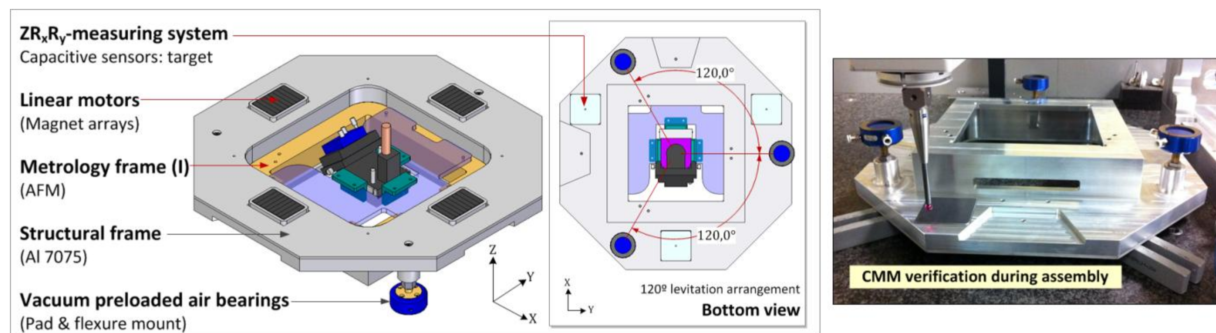

Figure 11. NanoPla moving platform: 3D-model and verification during assembly

It also incorporates the levitation system. The relative frictionless motion is possible with three vacuum preloaded air bearings as selected option in this case. Avoiding the difficult control task of maglev stages and despite of its low stiffness, vacuum preload offers a simpler and compact design, and no magnetic fields interaction. A preload force is created without increasing the weight of the system, besides the additional load of the moving part own weight. The air bearings selected were the New Way S205001 pad model. Their selection is a function of the weight that has to be lifted. Considering a value of less than 15 kg (for the moving platform), three air bearings with 50 mm diameter are adequate also for compactness. According to the datasheet, the ideal load for each of them is 45 N for air supply conditions of 0.41 MPa (input pressure) and 15 in Hg (input vacuum). Recommended by the manufacturer, these values are the used in NanoPla scheme. As fastening elements commercial flexures are used also of New Way to connect the embedded air bearing pad and the moving part through the assembly screw. Made of aluminum, they are capable to provide bi-directional stiffness because of the two-axis flexure hinge.

The operating requirements of the levitation system have been also evaluated. A similar setup has been defined with three air bearings (120º equally spaced) and three capacitive sensors for measuring vertical relative displacements. The probed air bearing stiffness of 11 N/µm is similar to the information

provided by the manufacturer (13 N/μm) by applying the recommended working conditions of input air and vacuum pressure (0.41 MPa and 15 in Hg, respectively) and load (45 N, ideal vs. 43.4 N of the experimental test). Discrepancies are notable in the air gap: 5 μm (datasheet) vs. 3.6 μm (test). This can be justified considering the different guide surface (different roughness) and unbalanced loads during the test (detected from the readouts of the three capacitive sensors). Thereby, it can be concluded that the levitation stability depends on the air supply condition, the fastening element and the delicate parallel alignment of the three pads during assembly.

The targets of the capacitive sensors are also located underneath this part. The distance between target and probe is related to the sensor range. The right positioning and parallelism of the three target planes has been characterized by a CMM (see Figure 11). The co-planarity error obtained is around 15 μm.

3.3.2 Moving metrology frame (I)

In the center of the moving platform the metrology frame (I) is placed, which it is illustrated in Figure 12. It integrates the AFM head and the plane mirrors over a squared frame. As in the static one, the final material of this part will be Zerodur, but in this first prototype, aluminum was used instead. Two Zerodur plane mirrors perpendicularly oriented (in X and Y) complete the laser measuring system as reflectors. During the assembly of this platform the squareness between these two mirrors in the plane XY was determined by measuring it in a CMM, obtaining a relative angle of 90.0374º.

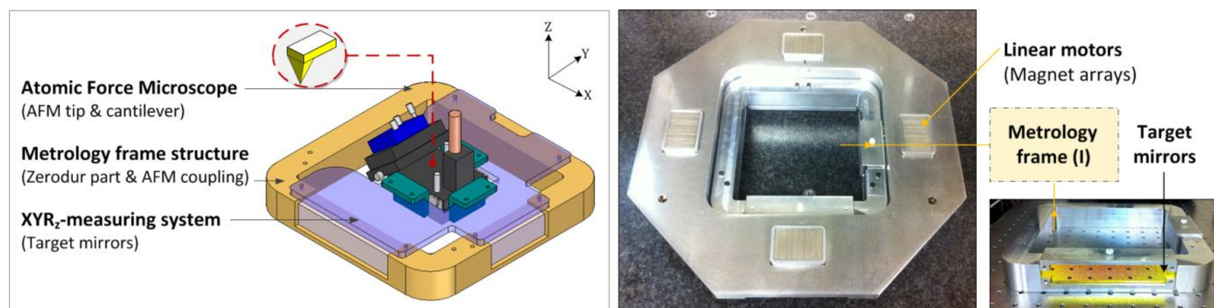

Figure 12. NanoPla metrology frame (I): components

The design of the stage has been oriented to allow the integration of different tools. However, its first application is focused on the surface topography characterization at atomic scale of samples whit relative big planar areas. Then, the initial considered tool will be an atomic force microscope developed by Nanotec Electrónica S.L. Its compact design and the open and modular control of Dulcinea electronics facilitate interfacing with the AFM or even others SPM future systems. Thus, the selected commercial solution gives advantages to attain a stage for multiple applications. Its compact design and open modular control are a clear advantage in this case. The AFM is also attached to this metrology frame in a position that meets the Abbe requirement with respect to the laser beams.

Due to the demanding requirements of the AFM measurement, the accurate displacement during scanning is assured with a commercial fine stage: NPXY100Z10A of nPoint and C-300 series controller. Different systems can be easily integrated or the available sample size can be increased. It will be supported by three micrometer screws DM-13L of Newport. The aim of this support for the short range stage is to provide not only the Z-coarse displacements of the sample, but also angular adjustments. Hence, it is possible to characterize relative height samples and motorize one of the screws for the approaching AFM operation.

3.4. Auxiliary systems

Once the laser interferometer scheme is used to measure relative in-plane motions, a homing system is required to establish a global reset. In addition, it will serve as a reference for linear motor phasing and error mapping. According to [11] in MAPS, three identical sensors can compose the homing system. Each one consists of two main parts: coarse zero (a pair of photo-micro-sensors and one symmetric graduated sheet) and fine homing (a combined scheme of LED-PSD). The design of the required electronic control circuit, component selection, and experimental tests for the NanoPla stage have been presented in [62]. The results show very different sensitivities that make appropriate the

combination of both tested systems for the application (PSD set-up ±0.76 µm/mV and photo-micro-sensors ±15 µm/mV). They will be included after validation of the XY-positioning performance results.

Isolation issues include vibration sources (environmental and acoustic noise) and temperature stability. Two are the included as auxiliary systems: a vibration isolation table and the laboratory where the stage works. The stage rests in a passive vibration isolation system (TMC High Performance Lab Table 900X1200X100) and is placed in a small metrology laboratory with controlled conditions. Once the system would be tested, considered additional measures are in the line of installing an extra enclosure for the machine as acoustic isolation and second controlled environment. This second thermal environment would use a more precise heat exchange system (i.e. water cooler covering the enclosure walls) in a smaller volume. However, both improvements should be in agreement with the tradeoff between the lack of heat dissipation when good acoustic isolation occurs.

3.5. Design validation

The first step of the design validation is based on mechanical simulations. Structural static and modal analyses have been carried out by the FEA software ANSYS®. The aim was to obtain an optimal prototype to be manufactured and assembled in terms of stiffness. In addition this simulation allowed some improvements in the design to finally meet the rigid-body behavior requirement, obtaining maximum deviations in the metrology frames of less than 13 nm.

Once defined the prototype geometry, error reduction and compensation methodologies can be applied. The information obtained from the experimental tests of the components and the mathematical error model allowed the development of an error budget of the whole system. The error budget is a well-established and advantageous technique for design improvement before manufacturing and initializing the system. Its utility is based on the study and quantification of the different error sources (contributions and their propagation around the metrology loop).

An error budget study for the 2D-nanopositioning stage final prototype is presented in [8]. A temperature control of ±0.1°C results in a maximum positioning error for the developed NanoPla stage, i.e., 41 nm, 36 nm and 48 nm in X-, Y- and Z-axis, respectively. These values are comparable to other similar stages. Our two main references MAPS and SAMM presents a similar error budget methodology in [11,18], respectively. For this reason they are here compared. Their design has been also based on an error budget with an analogous geometric mathematical model. In addition, both stages are similar in travel ranges and aimed accuracy, so that we dispose of comparable data. The different contributions are shown in Table 2, whose expressed errors are according to ASME B5.54 standard. The final error vector is a function of the mathematical model considered in the respective publications. In comparison, similar results show that the system design has been optimized in terms of positioning deviations. In all cases, the measurement deviations obtained demonstrate the important influence of the working environmental conditions, the flatness error of the plane mirror reflectors and the accurate manufacture and assembly of the components of the metrology loop. Thus, improvement measures should be established in those lines. Reversal techniques may be implemented to reduce target mirror flatness and orthogonality. In the SAMM case that leads to an error vector of 9.3 nm, 6.3 nm and 5.9 nm in X-, Y- and Z-axis, respectively [18]. The use of a better temperature-controlled chamber may help to reduce the effects of material thermal expansion and changes in the refractive index of air.

Table 2. Design validation by error budget results comparison

Regarding the nanopositioning stage here designed, the calibration routine should be firstly focused on the instrument modelling, i.e. the AFM over the long range moving platform. Calibration of SPMs has been already studied, with the aim of setting the basis for standardized procedures to assure traceability [63]. However, the problems at this working scale are the lack of procedures and non-availability of physical transfer standards. Considering artefacts, different commercial standards are currently available and new structures have been manufactured as more cost-effective solutions [64]. In view of the calibration technique, the self-calibration method becomes an interesting solution for these nanopositioning applications [65,66]. According to [66], the performance of the calibration is only limited by the instruments stability. Thus, this method based on multiple positions and orientations of a non-calibrated artefact could be a suitable solution for the NanoPla calibration task. With this aim,

preliminary works to obtain an effective and robust algorithm have been based on a similar setup that uses plane mirror laser interferometers as a 2D-sensor system [67].

4. Conclusions and future work

This paper presents a novel device for large range nanopositioning based on a three-layer architecture, whose components, arrangement and measurement strategy have been thoroughly justified. This architecture, the careful application of precision engineering principles and the design optimization and validation by an error budgeting technique have resulted in a compact system able to position in a 50 mm x 50 mm range with a 10 nm resolution. Since the system has been created to be combined with different devices (e.g. AFM topographic surface evaluation), this modularity provides it a wide field of possible applications in micro-metrology and micro-manufacturing.

Future specific tasks involve the integration of the complete 2D-control development and self-calibration procedure definition. The linear motor control strategy should be defined and implemented in the used hardware for the 1D- and 2D-cases. To complete the control loop, the sensor system should communicate with the actuators to provide accurate positioning. Once assured the control positioning task, the installation and calibration of a specific 2.5D-tool is planned to characterize the micro-geometry of relative big surfaces.

Acknowledgements

This work was funded by the Spanish government project DPI2010-21629-C02-01 "*NanoPla*" and DGA-FSE and the University of Zaragoza project UZ2014-TEC-05, with the collaboration of the DGA-FSE. Special thanks to the Center for Precision Metrology at the University of North Carolina Charlotte (UNC Charlotte) for its collaboration in this work, and the "*Consejo Nacional de Ciencia y Tecnología (CONACYT)*" from the government of Mexico which sponsored the second author.

References

[1] E. Manske, G. Jäger, T. Hausotte, R. Füßl, Recent developments and challenges of nanopositioning and nanomeasuring technology, Meas. Sci. Technol. 23 (2012) 074001. doi:10.1088/0957-0233/23/7/074001.

[2] W. Gao, S.W. Kim, H. Bosse, H. Haitjema, Y.L. Chen, X.D. Lu, et al., Measurement technologies for precision positioning, CIRP Ann. - Manuf. Technol. 64 (2015) 773–796. doi:10.1016/j.cirp.2015.05.009.

[3] L. Li, M. Hong, M. Schmidt, M. Zhong, A. Malshe, B. Huis In'Tveld, et al., Laser nano-manufacturing - State of the art and challenges, CIRP Ann. - Manuf. Technol. 60 (2011) 735–755. doi:10.1016/j.cirp.2011.05.005.

[4] F.Z. Fang, X.D. Zhang, A. Weckenmann, G.X. Zhang, C. Evans, Manufacturing and measurement of freeform optics, CIRP Ann. - Manuf. Technol. 62 (2013) 823–846. doi:10.1016/j.cirp.2013.05.003.

[5] A. Balasubramanian, M.B.G. Jun, R.E. DeVor, S.G. Kapoor, A Submicron Multiaxis Positioning Stage for Micro- and Nanoscale Manufacturing Processes, J. Manuf. Sci. Eng. 130 (2008) 031112. doi:10.1115/1.2917315.

[6] S. Ducourtieux, B. Poyet, Development of a metrological atomic force microscope with minimized Abbe error and differential interferometer-based real-time position control, Meas. Sci. Technol. 22 (2011) 094010. doi:10.1088/0957-0233/22/9/094010.

[7] H.N. Hansen, K. Carneiro, H. Haitjema, L. De Chiffre, Dimensional micro and nano metrology, CIRP Ann. - Manuf. Technol. 55 (2006) 721–743. doi:10.1016/j.cirp.2006.10.005.

[8] M. Torralba, J. Yagüe-Fabra, J. Albajez, J. Aguilar, Design Optimization for the Measurement Accuracy Improvement of a Large Range Nanopositioning Stage, Sensors. 16 (2016) 84. doi:10.3390/s16010084.

[9] C. Werner, A 3D translation stage for metrological AFM, Eindhoven University Technology, 2010.

[10] P. Klapetek, M. Valtr, M. Matula, A long-range scanning probe microscope for automotive reflector optical quality inspection, Meas. Sci. Technol. 22 (2011) 094011. doi:10.1088/0957-0233/22/9/094011.

[11] R. Fesperman, O. Ozturk, R. Hocken, S. Ruben, T.C. Tsao, J. Phipps, et al., Multi-scale Alignment and Positioning System - MAPS, Precis. Eng. 36 (2012) 517–537. doi:10.1016/j.precisioneng.2012.03.002.

[12] J.A. Kramar, Nanometre resolution metrology with the Molecular Measuring Machine, Meas. Sci. Technol. 16 (2005) 2121–2128. doi:10.1088/0957-0233/16/11/001.

[13] UA3P, (n.d.).

[14] J.A. Kim, J.W. Kim, C.S. Kang, T.B. Eom, Metrological atomic force microscope using a large range scanning dual stage, Int. J. Precis. Eng. Manuf. 10 (2009) 11–17. doi:10.1007/s12541-009-0087-z.

[15] C.H. Liu, W.Y. Jywe, Y.R. Jeng, T.H. Hsu, Y. tsung Li, Design and control of a long-traveling nano-positioning stage, Precis. Eng. 34 (2010) 497–506. doi:10.1016/j.precisioneng.2010.01.003.

[16] C. Yang, G.L. Wang, B.S. Yang, H.R. Wang, Research on the structure of high-speed large-scale ultra-precision positioning system, in: Nano/Micro Eng. Mol. Syst. NEMS 2008. 3rd IEEE Int. Conf., 2008: pp. 9–12.

[17] S. Hesse, C. Schäffel, H.-U. Mohr, M. Katzschmann, H.-J. Büchner, Design and performance evaluation of an interferometric controlled planar nanopositioning system, Meas. Sci. Technol. 23 (2012) 074011. doi:10.1088/0957-0233/23/7/074011.

[18] M. Holmes, R. Hocken, D. Trumper, Long-range scanning stage: A novel platform for scanned-probe microscopy, Precis. Eng. 24 (2000) 191–209. doi:10.1016/S0141-6359(99)00044-6.

[19] T.-T. Chung, C.-H. Chu, K.-C. Fan, J.-Y. Yen, Development of a Nano-Positioning Planar Motion Stage, in: International Conference on Mechanical and Electronics Engineering (ICMEE), 2012: pp. 122–126.

[20] A.H. Slocum, S. of M. Engineers, Precision machine design, Society of Manufacturing Engineers, Dearborn Michigan, 1992.

[21] P. Schellekens, N. Rosielle, H. Vermeulen, M. Vermeulen, S. Wetzels, W. Pril, Design for Precision: Current Status and Trends, CIRP Ann. - Manuf. Technol. 47 (1998) 557–586. doi:10.1016/S0007-8506(07)63243-0.

[22] H. Van Brussel, J. van Eijk, H. Spaan, E. Brinksmeier, Precision Engineering: The European Way, in: ASPE 2008 Annu. Meet., n.d.

[23] W. Wang, Z. Zhu, Z. Chen, R.J. Hocken, A piezodriven three dimensional micropositioning stage for nano-manufacturing, 10th Int. Symp. Meas. Qual. Control 2010, ISMQC 2010. (2010) 563.

[24] L. CX, G. GY, Y. MJ, Z. LM, Design, analysis and testing of a parallel-kinematic high-bandwidth XY nanopositioning stage., Rev. Sci. Instrum. 84 (2013) 125111.

[25] G. Shan, Y. Li, L. Zhang, Z. Wang, Y. Zhang, J. Qian, Contributed Review: Application of voice coil motors in high-precision positioning stages with large travel ranges, Rev. Sci. Instrum. 86 (2015) 101501. doi:10.1063/1.4932580.

[26] W.Y. Jywe, Y.R. Jeng, Y.F. Teng, H.S. Wang, C.H. Wu, Development of the nano-measuring machine stage, in: IECON Proc. (Industrial Electron. Conf., 2007: pp. 2970–2973. doi:10.1109/IECON.2007.4460035.

[27] W. Kim, D.L. Trumper, High-precision magnetic levitation stage for photolithography, Precis. Eng. 22 (1998) 66–77. doi:10.1016/S0141-6359(98)00009-9.

[28] W. jong Kim, S. Verma, H. Shakir, Design and precision construction of novel magnetic-levitation-based multi-axis nanoscale positioning systems, Precis. Eng. 31 (2007) 337–350. doi:10.1016/j.precisioneng.2007.02.001.

[29] S. Dejima, W. Gao, H. Shimizu, S. Kiyono, Y. Tomita, Precision positioning of a five degree-of-freedom planar motion stage, Mechatronics. 15 (2005) 969–987. doi:10.1016/j.mechatronics.2005.03.002.

[30] T.T. Chung, C.H. Chu, H.F. Chian, C. Huang, K.C. Fan, J.Y. Yen, et al., Structural design and analysis of a nano-positioning planar motion stage, in: Proc. World Congr. Intell. Control Autom., Institute of Electrical and Electronics Engineers Inc, Department of Mechanical Engineering, National Taiwan University, Taipei, Taiwan, 2011: pp. 833–838. doi:10.1109/WCICA.2011.5970632.

[31] A.J. Fleming, A review of nanometer resolution position sensors: Operation and performance, Sensors Actuators, A Phys. 190 (2013) 106–126. doi:10.1016/j.sna.2012.10.016.

[32] S.K. Ro, J.K. Park, A compact ultra-precision air bearing stage with 3- DOF planar motions using electromagnetic motors, Int. J. Precis. Eng. Manuf. 12 (2011) 115–119. doi:10.1007/s12541-011-0014-y.

[33] W. Gao, S. Dejima, H. Yanai, K. Katakura, S. Kiyono, Y. Tomita, A surface motor-driven planar motion stage integrated with an XYθZ surface encoder for precision positioning, Precis. Eng. 28 (2004) 329–337. doi:10.1016/j.precisioneng.2003.12.003.

[34] X. Li, W. Gao, H. Muto, Y. Shimizu, S. Ito, S. Dian, A six-degree-of-freedom surface encoder for precision positioning of a planar motion stage, Precis. Eng. 37 (2013) 771–781. doi:10.1016/j.precisioneng.2013.03.005.

[35] M.M.P.A. Vermeulen, P.C.J.N. Rosielle, P.H.J. Schellekens, Design of a High-Precision 3D-Coordinate Measuring Machine, CIRP Ann. - Manuf. Technol. 47 (1998) 447–450. doi:10.1016/S0007-8506(07)62871-6.

[36] Zeiss, (n.d.).

[37] J.K. v. Seggelen, NanoCMM: A 3D coordinate Measuring Machine with low moving mass for measuring small products in array with nanometer uncertainty, TU/e, 2007.

[38] G. Jäger, E. Manske, T. Hausotte, H.J. Büchner, Nanomeasuring and nanopositioning engineering, in: Fringe 2009 - 6th Int. Work. Adv. Opt. Metrol., 2009: pp. 390–397. doi:10.1007/978-3-642-03051-2-64.

[39] A. Rudolf, C. Mock, C. Walenda, R. Gloess, R. Liang, C. Schaeffel, et al., 6D Magnetic levitation positioning system with compact integrated 6D sensor, in: Euspen International Conference, 2012: pp. 399–403.

[40] PIMag® 6D Magnetic Levitation, (n.d.).

[41] B.J. Eves, Design of a large measurement-volume metrological atomic force microscope (AFM), Meas. Sci. Technol. 20 (2009) 084003. doi:10.1088/0957-0233/20/8/084003.

[42] T. Rujil, Ultra Precision Coordinate Measuring Machine. Design, Calibration and Error Compensation., Delft University of Technology, 2001.

[43] R.L. Donker, I. Widdershoven, D. Brouns, H.A.M. Spaan, Realization of Isara 400: a large measurement volume ultra-precision CMM, in: ASPE Annual Proceedings, Sesion III, Dimensional Metrology, 2009.

[44] ISARA 400, (n.d.).

[45] A.J. Hart, A. Slocum, P. Willoughby, Kinematic coupling interchangeability, Precis. Eng. 28 (2004) 1–15. doi:http://dx.doi.org/10.1016/S0141-6359(03)00071-0.

[46] S.T. Smith, Flexures: Elements of Elastic Mechanisms, CRC Press, 2000.

[47] M.C.J.M. Van Riel, E.J.C. Bos, F.G.A. Homburg, Design of a Low-cost CMM with Nanometer Uncertainty, in: 2010.

[48] K.C. Fan, Y. Fei, X. Yu, W. Wang, Y. Chen, Study of a noncontact type micro-CMM with arch-bridge and nanopositioning stages, Robot. Comput. Integr. Manuf. 23 (2007) 276–284. doi:10.1016/j.rcim.2006.02.007.

[49] H. Nouira, J.-A. Salgado, N. El-Hayek, S. Ducourtieux, A. Delvallée, N. Anwer, Setup of a high-precision profilometer and comparison of tactile and optical measurements of standards, Meas. Sci. Technol. 25 (2014) 044016. doi:10.1088/0957-0233/25/4/044016.

[50] K.H. Kim, M.G. Lee, D.M. Kim, D.G. Gweon, Control and Design of a Dual Servo with Fine 6-axis Stage, in: ASPE Annual Proceedings, Poster Session, 2003: pp. 187–190.

[51] Y.-M. Choi, D.-G. Gweon, A High-Precision Dual-Servo Stage Using Halbach Linear Active Magnetic Bearings, Ieee-Asme Trans. Mechatronics. 16 (2011) 925–931. doi:10.1109/TMECH.2010.2056694.

[52] A.J.M. Moers, M.C.J.M. Van Riel, E.J.C. Bos, Design and verification of the TriNano ultra precision CMM, in: 56th International Scientific Colloquium, 2011.

[53] G. Barbieri, C. Fantuzzi, R. Borsari, A model-based design methodology for the development of mechatronic systems, Mechatronics. 24 (2014) 833–843. doi:10.1016/j.mechatronics.2013.12.004.

[54] Object Management Group 2012 Systems modeling language specification, (n.d.).

[55] Y. Cao, Y. Liu, H. Fan, B. Fan, SysML-based uniform behavior modeling and automated mapping of design and simulation model for complex mechatronics, CAD Comput. Aided Des. 45 (2013) 764–776. doi:10.1016/j.cad.2012.05.001.

[56] A. Sinno, P. Ruaux, L. Chassagne, S. Topု, Y. Alayli, G. Lerondel, et al., Enlarged atomic force microscopy scanning scope: Novel sample-holder device with millimeter range, Rev. Sci. Instrum. 78 (2007) 95107. doi:10.1063/1.2773623.

[57] E.S. Buice, S.T. Smith, R.J. Hocken, Experimental evaluation of a dual-axis ultra-precision positioning stage for probe studies, in: Euspen Internacional Conference, 2008: pp. 368–371.

[58] H. Sawano, T. Gokan, H. Yoshioka, H. Shinno, A newly developed STM-based coordinate measuring machine, Precis. Eng. 36 (2012) 538–545. doi:10.1016/j.precisioneng.2012.02.007.

[59] H. Shinno, H. Yoshioka, K. Taniguchi, A newly developed linear motor-driven aerostatic X-Y planar motion table system for nano-machining, CIRP Ann. - Manuf. Technol. 56 (2007) 369–372. doi:10.1016/j.cirp.2007.05.086.

[60] D.L. Trumper, W. Kim, M.E. Williams, Design and analysis framework for linear permanent-magnet machines, IEEE Trans. Ind. Appl. 32 (1996) 371–379. doi:10.1109/28.491486.

[61] M. Torralba, J.A. Albajez, J.A. Yagüe, J.A. Aguilar, Preliminary Modelling and Implementation of the 2D-control for a Nanopositioning Long Range Stage, Procedia Eng. 132 (2015) 824–831. doi:10.1016/j.proeng.2015.12.566.

[62] R. Acero, J.A. Albajez, J.A. Yagüe-Fabra, M. Torralba, M. Valenzuela, J.J. Aguilar, Analysis and design of a homing sensor system for a 2D moving platform with nanometer resolution, in: Procedia Eng., 2013: pp. 183–192. doi:10.1016/j.proeng.2013.08.192.

[63] G. Wilkening, L. Koenders, Towards a Guideline for SPM Calibration., Nanoscale Calibration Stand. Methods Dimens. Relat. Meas. Micro Nanom. Range. (2005) 171–192.

[64] R. Leach, C. Giusca, M. Guttmann, P.-J. Jakobs, P. Rubert, Development of low-cost material measures for calibration of the metrological characteristics of areal surface texture instruments, CIRP Ann. - Manuf. Technol. (2015).

[65] Y.H. Jeong, J. Dong, P.M. Ferreira, Self-calibration of dual-actuated single-axis nanopositioners, Meas. Sci. Technol. 19 (2008) 045203. doi:10.1088/0957-0233/19/4/045203.

[66] M. Xu, T. Dziomba, G. Dai, L. Koenders, Self-calibration of scanning probe microscope: mapping the errors of the instrument, Meas. Sci. Technol. 19 (2008) 025105. doi:10.1088/0957-0233/19/2/025105.

[67] J.A. Yagüe-Fabra, M. Valenzuela, J.A. Albajez, J.J. Aguilar, A thermally-stable setup and calibration technique for 2D sensors, CIRP Ann. - Manuf. Technol. 60 (2011) 547–550. doi:http://dx.doi.org/10.1016/j.cirp.2011.03.058.

[68] J.L. Overcash, R.J. Hocken, C.G. Stroup Jr., Noise reduction and disturbance rejection at the sub-nanometer level, in: ASPE Annual Proceedings, Session VIII, Design of Precision Machines and Instruments, 2009: pp. 2765–2768.

Table 1. Nanopositioning stages overview. Design features

Refs	Research Institution/ Company	XY(Z)-range [mm]	XY-stage structure	Driving system	Motion system scheme	Scanning type strategy	Metrology loop XY-sensor	XY-Positioning resolution	XY-Positioning accuracy/error	Comments
NanoPla	University of Zaragoza (Spain)	50x50	Plane motion	Home-made LM VPL air bearing	Coarse + fine	Combined	Plane mirror laser interferometer	Goal: 10 nm	Goal: 25 nm	Three-layer architecture Inverted linear motors
[26]	National Formosa University (Taiwan)	20x20 (0.018)	Stacked motion	VCM (Linear guides)	Coarse + fine	Scanning sample	Plane mirror laser interferometer	-	X: 22 µm Y: 23 µm	Voice coil motors
[15]	National Formosa University (Taiwan)	300x300	Stacked motion	Servo motor (Linear guide, ball screws)	Coarse + fine	Scanning sample	Plane mirror laser interferometer	≈ 9.8 nm	X: ±10 nm Y: ±10 nm (high speed 34.6 mm/s)	Traditional lead screws + piezostage High velocity (34.6 mm/s)
[16]	Xi'an Jiaotong University (China)	300x300	Stacked motion	LM U-shaped	Coarse + fine	Scanning sample	Retroreflector laser interferometer	100 nm	< 3 µm	Linear motors High velocity (500 mm/s)
[11]	University of North Carolina (USA)	10x10 (1.5)	Plane motion	Home-made LM VPL air bearing	Long range	Scanning sample	Plane mirror laser interferometer	Goal < 1 nm (Tested 0.15 nm)	Goal: 2 nm	**MAPS** Home-made LM
[27]	SatCon Technology Corp MIT (USA)	50x50 (0.4)	Plane motion	Home-made LM (maglev)	Long range	Scanning sample	Plane mirror laser interferometer	< 10 nm	-	Maglev Wafer stepper
[28]	Texas A&M University (USA)	5x5 (0.5)	Plane motion	Novel 2D-motor (maglev)	Long range	Scanning sample	Plane mirror laser interferometer	< 3 nm	Command tracking errors ±10 nm	Maglev Actuator design
[18,68]	University of North Carolina MIT (USA)	25x25 (0.1)	Plane motion	Home-made LM (maglev)	Coarse + fine	Scanning sample	Plane mirror laser interferometer	Goal: 0.1 nm	Goal: 10 nm Positioning noise < 0.6 nm (3σ)	**SAMM** Maglev Damping: oil floation
[29]	Tohoku University (Japan)	200x200	Plane motion	LM Magnetic preloaded air bearing	Long range	Scanning sample	2D-angle grid surface encoder (home-made)	50 nm	Deviation error: ±460 nm (3σ)	Air bearings: magnetically preloaded
[19,30]	National Taiwan University (Taiwan)	50x50	Plane motion	LM Face to face air bearings preload	Long range	Scanning sample	2D-surface grid encoder	Goal: 100 nm	Goal: 1 µm	Air bearings: Opposed air bearings preload arrangement
[17]	Ilmenau University of Technology IMMS GmbH. (Germany)	Ø100	Plane motion	Linear drive units (flat coils) VPL air bearing	Long range	Scanning sample	Plane mirror laser interferometer	0.5 nm (tested)	Servo error (tested) < 1.3 nm	Air bearings: vacuum preloaded
[32]	Korea Institute of Machinery and Materials (South Korea)	20 x 20	Plane motion	LM Magnetic preloaded air bearing by the LM	Long range	Scanning sample	2D-surface grid encoder (commercial)	20 nm	100 nm repeatability	2D-grid encoder (commercial)
[33,34]	Tohoku University (Japan)	40 x 40	Plane motion	LM	Long range	Scanning sample	2D- and 6D-surface encoder (home-made)	2 nm	X: ±6 nm Y: ±7 nm	Home-made surface encoders
[35,36]	Zeiss	135x135 (100)	(*) Plane motion Particular design	LM	Long range	Scanning probe	Linear encoder	2.5 nm	250 nm	**F25** 1D-linear encoders
[37]	Eindhoven University of Technology (The Netherlands)	50x50 (4)	(*) Plane motion Particular design	VCM	Long range	Scanning probe	Linear encoder	1 nm (optical linear encoders)	X: ±4 nm Y: ±3 nm Volumetric: 13 nm (k=1)	1D-linear encoders Asymmetric kinematic configuration
[1,38]	Ilmenau University of Technology SIOS Meβtechnik GmbH. Ilmenau (Germany)	25x25 (5)	Stacked motion	VCM Linear ball-bearing guides	Long range	Scanning sample	Plane mirror laser interferometer (one measuring beam)	0.1 nm	Stability ≈ 0.3 nm (closed-loop positioning control)	**NMM-1** Plane mirror laser interferometer
[39,40]	IMMS Physik Instrumente (Germany)	100x100 (0.5)	Plane motion	LM	Long range	Scanning sample	2D-surface grid encoder (optical incremental)	10 nm	Stability (XY) 3.5 nm	Compact 6D-head: optical grid encoder + capacitive sensors
[41]	National Research Council (Canada)	100x100 (15) (*)AFM 40x40 (6)	Stacked motion	LM	Coarse + fine	Scanning sample	Plane mirror laser interferometer	0.3 nm (Fine stage closed-loop resolution)	Goal: 1 nm (k=1)	Auto-collimators Two commercial stacked stages
[42–44]	IBS Precision Engineering, Eindhoven (The Netherlands)	400x400 (100)	Stacked motion	LM U-shaped	Long range	Combined XY-Z	Plane mirror laser interferometer	-	71 nm (k=2) 3D-uncertainty: 109 nm (k=2)	**ISARA** Metrology frame definition
[47,48]	Hefei University of Technology (China) National Taiwan University (Taiwan)	25x25 (10)	Stacked motion	LM ultrasonic (AC/DC for coarse and fine motion)	(*) Coarse + fine	Combined XY-Z	Linear encoder (hologram grating scales)	1 nm	20 nm (after error compensation)	Co-planar concept

Table 1. Nanopositioning stages overview. Design features (cont.)

Refs	Research Institution/ Company	XY(Z)-range [mm]	XY-stage structure	Driving system	Motion system scheme	Scanning type strategy	Metrology loop XY-sensor	XY-Positioning resolution	XY-Positioning accuracy/error	Comments
[49]	Laboratoire National de Métrologie et d'Essais (France)	50x50 (100)	Stacked motion	High-precision guiding systems	Long range	Scanning sample	Plane mirror laser interferometer	-	30 nm	CMM-structure
[50]	Korea Advanced Institute of Science and Technology (South Korea)	200x200	Stacked motion	LM Air bearings	Coarse + fine	Scanning sample	Coarse: linear encoder Fine: plane mirror laser interferometer	-	-	Double H-structure
[51]	Korea Advanced Institute of Science and Technology (South Korea)	300x300	Stacked motion	LM U-shaped Linear ball bearings	Coarse + fine	Scanning sample	Coarse: linear encoder Fine: plane mirror laser interferometer	5 nm	Stability: X: ±10 nm Y: ±15 nm	H-structure
[14]	Korea Research Institute of Standards and Science (South Korea)	200x200	Stacked motion	Servo motor and lead screw (Precision surfaces with guide bars)	Coarse + fine	Combined XY-Z	Plane mirror laser interferometer	Coarse < 100 nm Fine ≈ 1 nm	≈ 60 nm	Cross structure
[52]	Xpress Precision Engineering Eindhoven University of Technology (The Netherlands)	$64\ cm^3$	(*) Tripod	Three 1D-translation stages	Long range	Scanning sample	Linear encoders	-	Goal: 100 nm (k=2)	Trinano Tripod
[9]	Eindhoven University of Technology (The Netherlands)	1x1 (1)	(*) Tripod	VCM (Elastic parallel guides)	Long range	Scanning sample	Differential interferometer s	Goal < 1 nm	≤ 10 nm	Tripod
[12]	National Institute of Standards and Technology (USA)	50x50	(*) Stacked motion	Piezo-ceramic stepper motors Slideways	(*) Coarse + fine	(*) Combined X-Sample YZ-Probe	Plane mirror laser interferometer	-	Goal: 1 nm combined uncertainty (point-to-point)	Isolation Separated stacked coarse+fine for X and Y
[10]	Czech Metrology Institute (Czech Republic)	10x10 (20 µm)	Stacked motion	VCM Crossed roller bearing stages	Long range	Scanning sample	Plane mirror laser interferometer	10 nm	Position error root mean square < 5 nm	Long range AFM
[56]	LISV, University of Versailles (France)	50x50	Stacked motion	LM	Coarse + fine	Scanning sample	Plane mirror laser interferometer	Coarse 10 nm (XY separately) Fine < 1 nm	-	Coarse + fine Different scanning modes
[57]	University of North Carolina (USA)	50x50 (4 µm)	Stacked motion	Brushless DC motor feedscrew Slideways	Coarse + fine	Scanning sample	Plane mirror laser interferometer	Goal < 1 nm	Standard deviations Coarse ≈ 2.5 µm Fine < 3.2 nm	Coarse+fine
[13]	Panasonic Corp.		Stacked motion	LM	Long range	Scanning probe	Plane mirror laser interferometer	-	Measurement errors (XY)	**UA3P** Scanning probe
	UA3P-300	30x30 (20)							Up to 100mm within 0.05µm	
	UA3P-4	100x100 (35)							Up to 100mm within 0.05µm	
	UA3P-5	200x200 (45)							Up to 200mm within 0.1µm	
[58,59]	Precision and Intelligent Laboratory Tokyo Institute of Technology (Japan)	18x18 (10)	Plane motion	VCM VPL air bearing	Long range	Combined XY-Z	Plane mirror laser interferometer	1 nm	Repeatability < 50 nm (wide range scans of spherical surfaces)	Combined scanning

Table 1 (Notes)

- Nanopositioning stages in order of appearance in subsection 2.3.
- If there is no information about the tool position, it is understood that the table or moving part locates the sample (scanning sample).
- Abbreviations: LM (linear Motor); VCM (Voice Coil Motor); VPL (Vacuum Preloaded)

Table 2. Design validation by error budget results comparison

	Geometric error	**MAPS** [11] 10x10 mm^2	**SAMM** [18] 25x25 mm^2	**NanoPla** [8] 50x50 mm^2
[nm]	δ_x **(X)**	18.50	2.10	16.14
	δ_x **(Y)**	2.40	32.0	
	δ_x **(Z)**	0.02	32.0	
	δ_y **(X)**	2.40	32.0	16.14
	δ_y **(Y)**	18.50	2.1	
	δ_y **(Z)**	0.02	32.0	
	δ_z **(X)**	0.00	32.0	19.05
	δ_z **(Y)**	0.00	32.0	
	δ_z **(Z)**	2.00	1.5	
[nrad]	ε_x	71.6	60.0	15.4
	ε_y	71.6	60.0	15.4
	ε_z	464.0	80.0	286.0
[μrad]	α_{xy}	24.24	14.54	1.09
	α_{yz}	24.24	24.24	1.14
	α_{zx}	24.24	24.24	1.31
Final error [nm]	Δ**X**	**72**	**218**	**41**
	Δ**Y**	**20**	**37**	**36**
	Δ**Z**	**2**	**36**	**48**

Figure1
Click here to download high resolution image

XY-Positioning error (nm)
1000
100
10
1
0 50 100 150 200 250 300
XY-Range (mm)
High accuracy but short range or complex
Medium range and accuracy but big and expensive machines
Long range but limited accuracy
[9] [10] [11] [12] Ultra-high-precision CMMs
[13] [14] [15] [16] Stacked stages
NanoPla [17] [18] [19] Plane stages

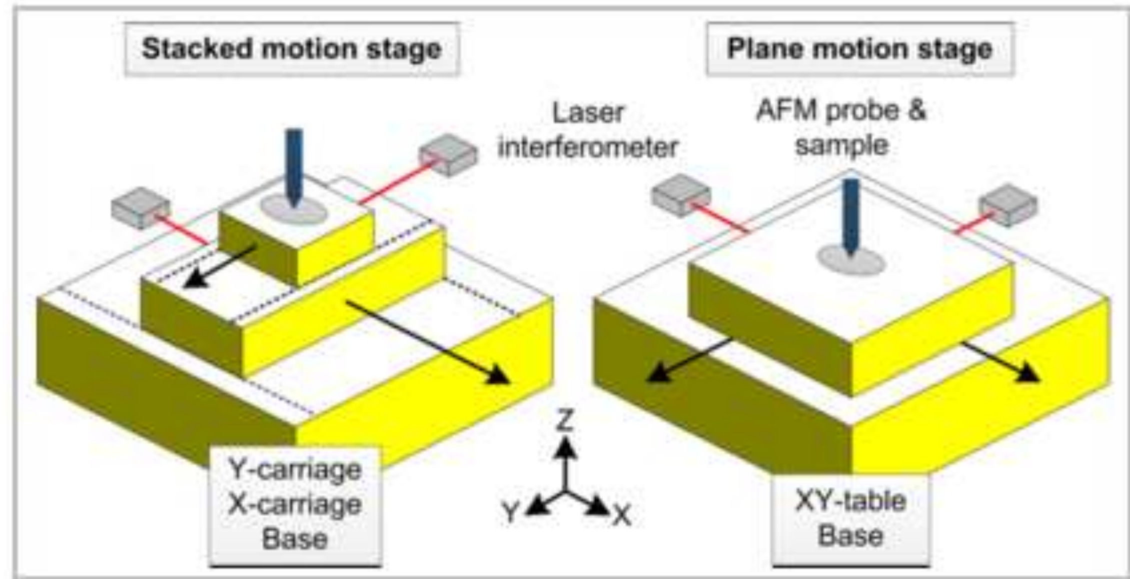

Figure2

Click here to download high resolution image

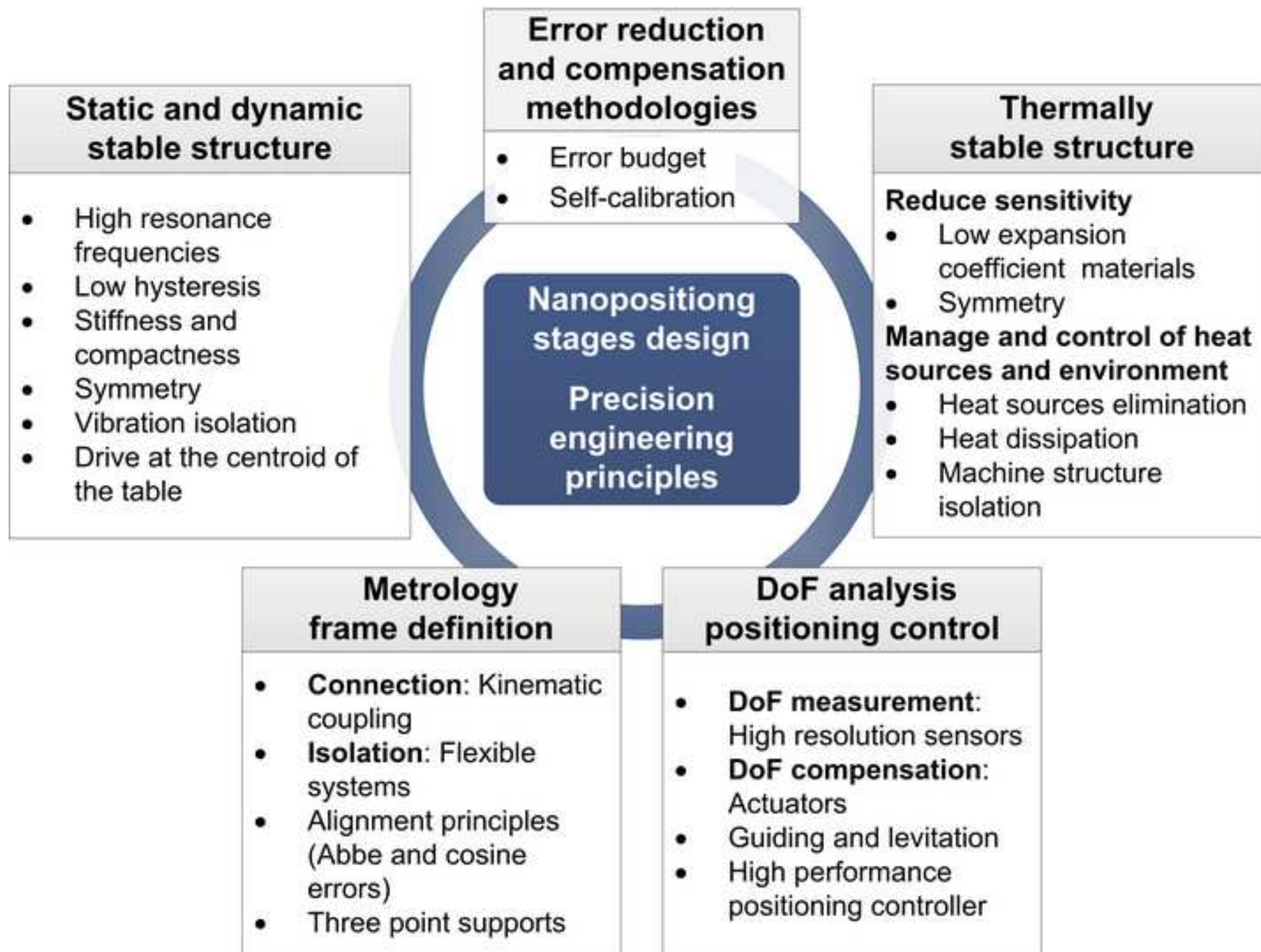

Figure3
Click here to download high resolution image

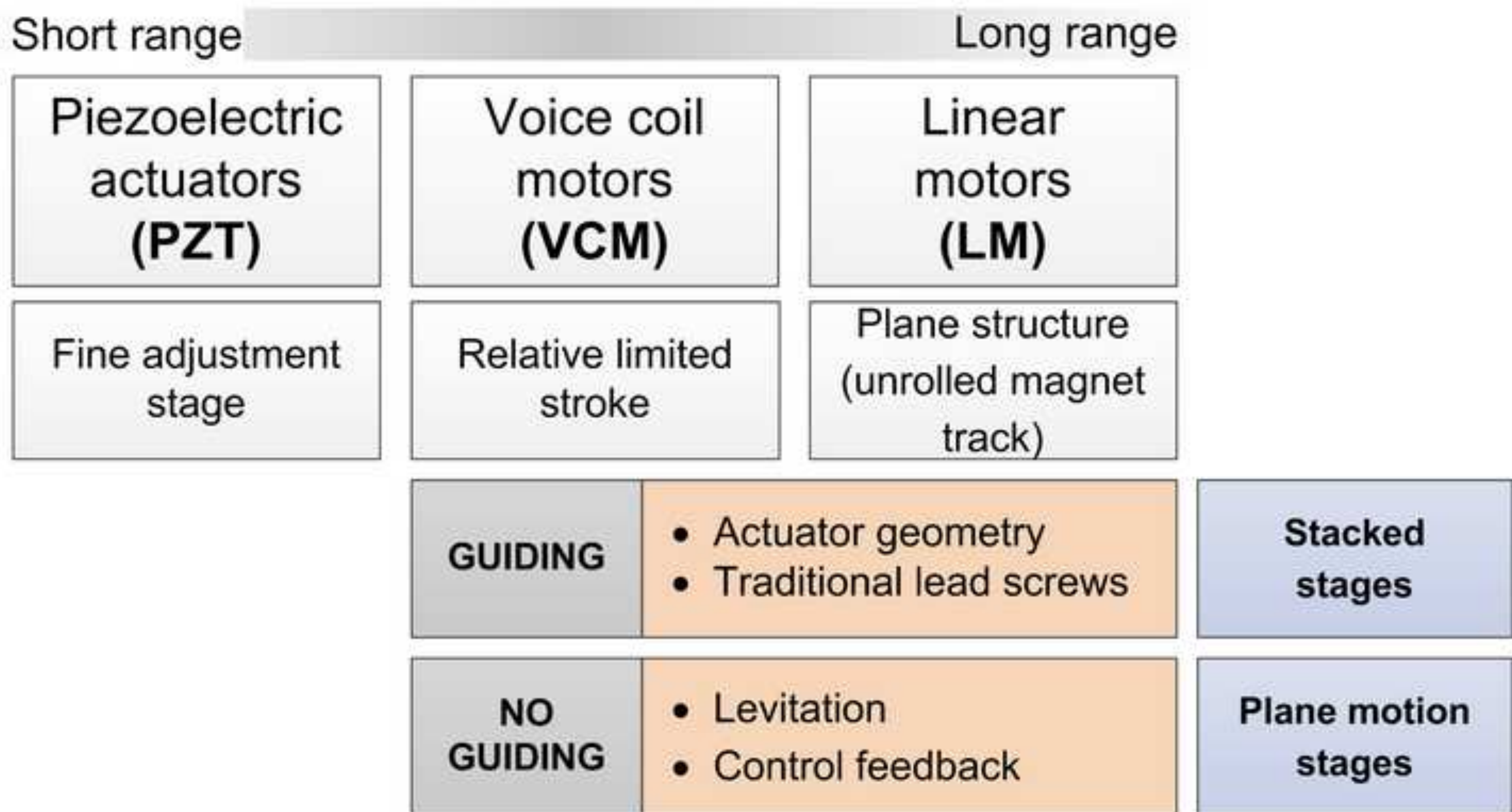

Figure4
Click here to download high resolution image

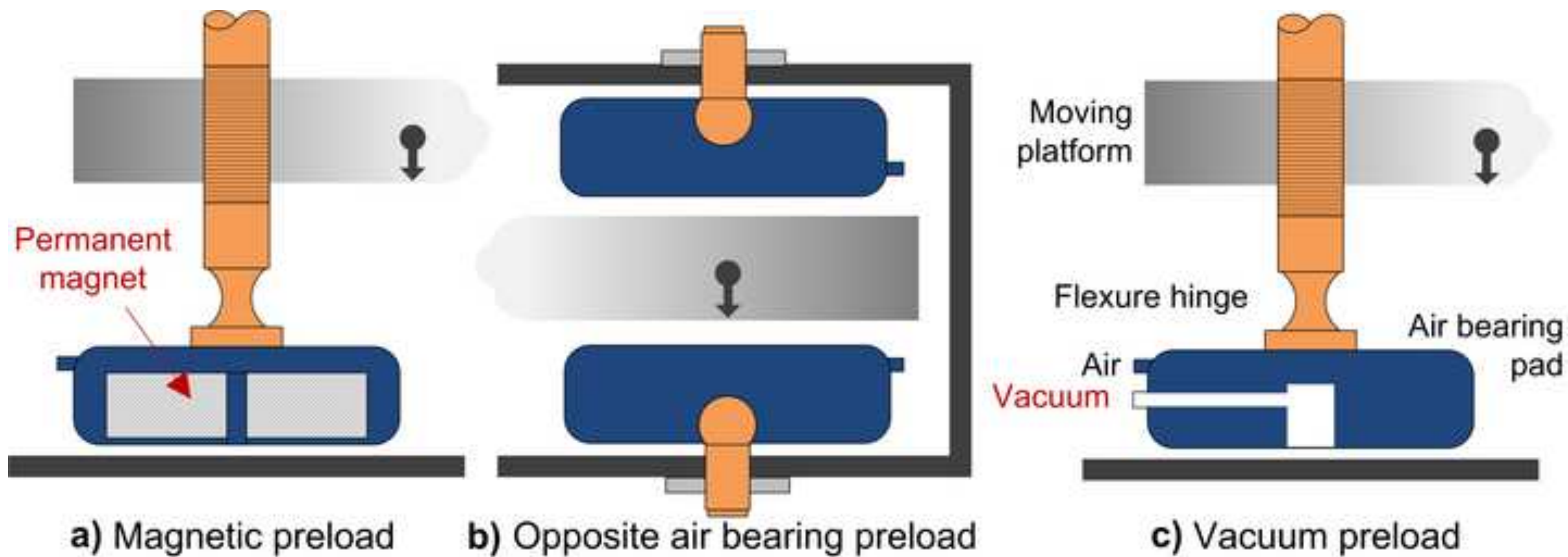

Figure5
Click here to download high resolution image

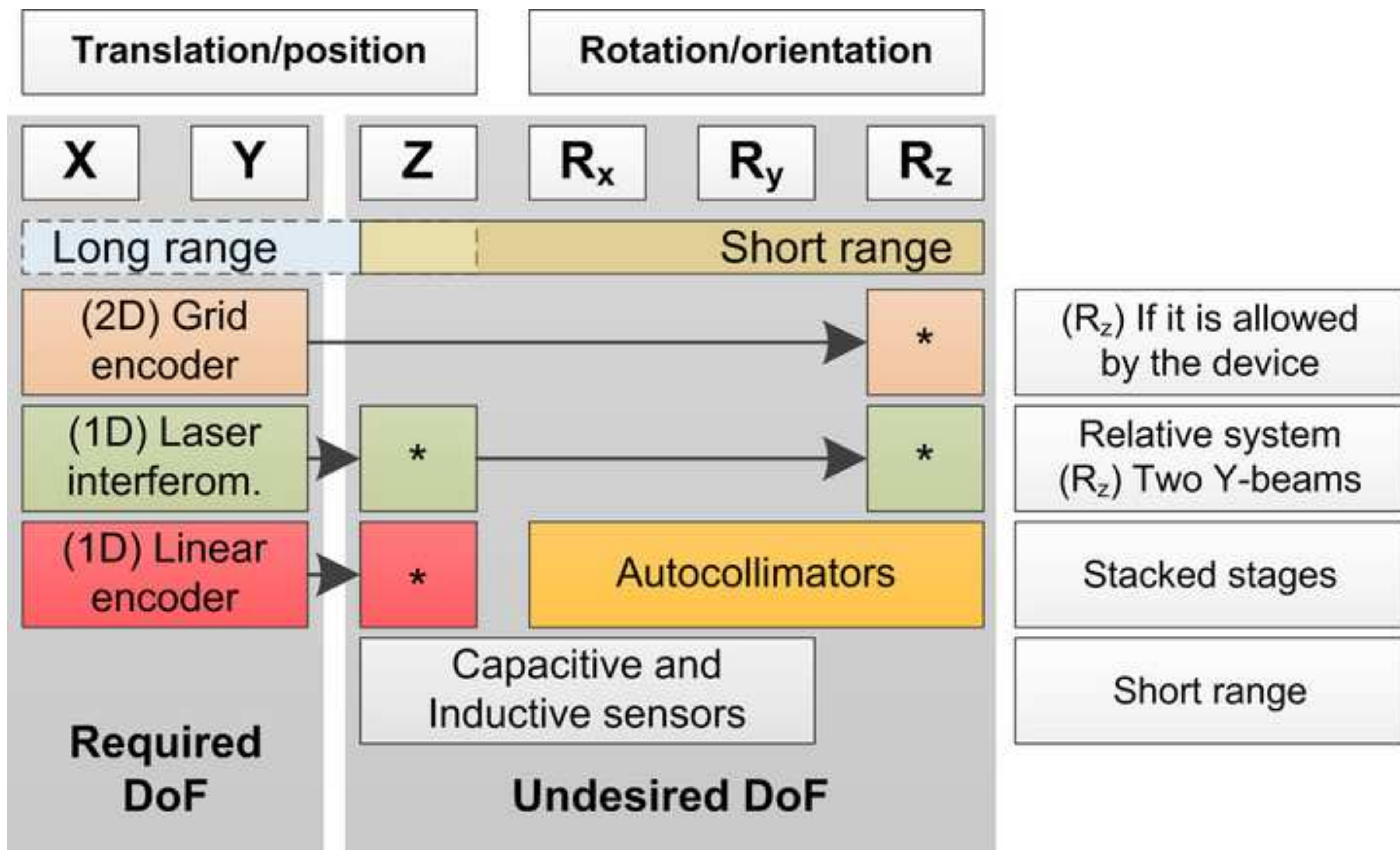

Figure6

Click here to download high resolution image

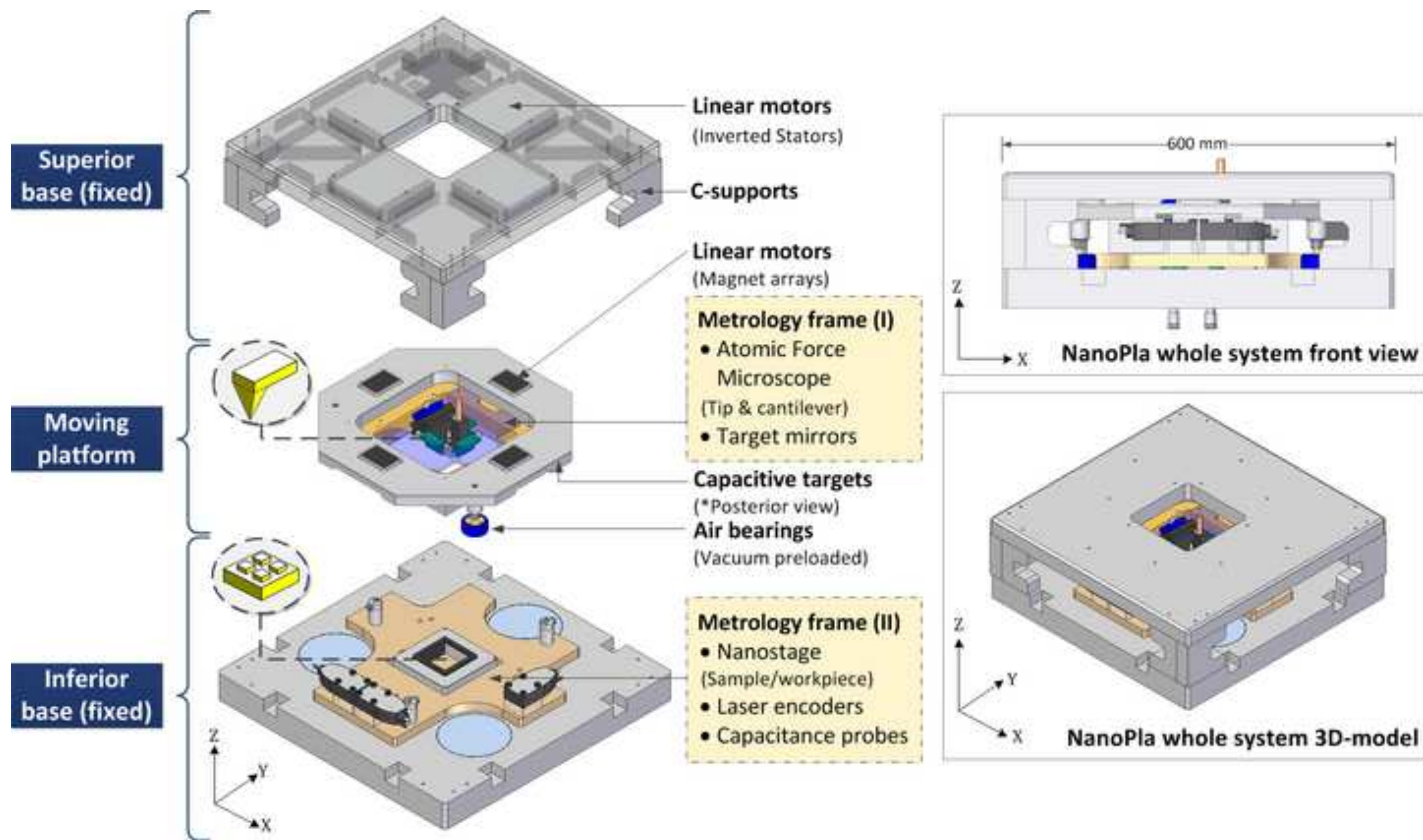

Figure7

Click here to download high resolution image

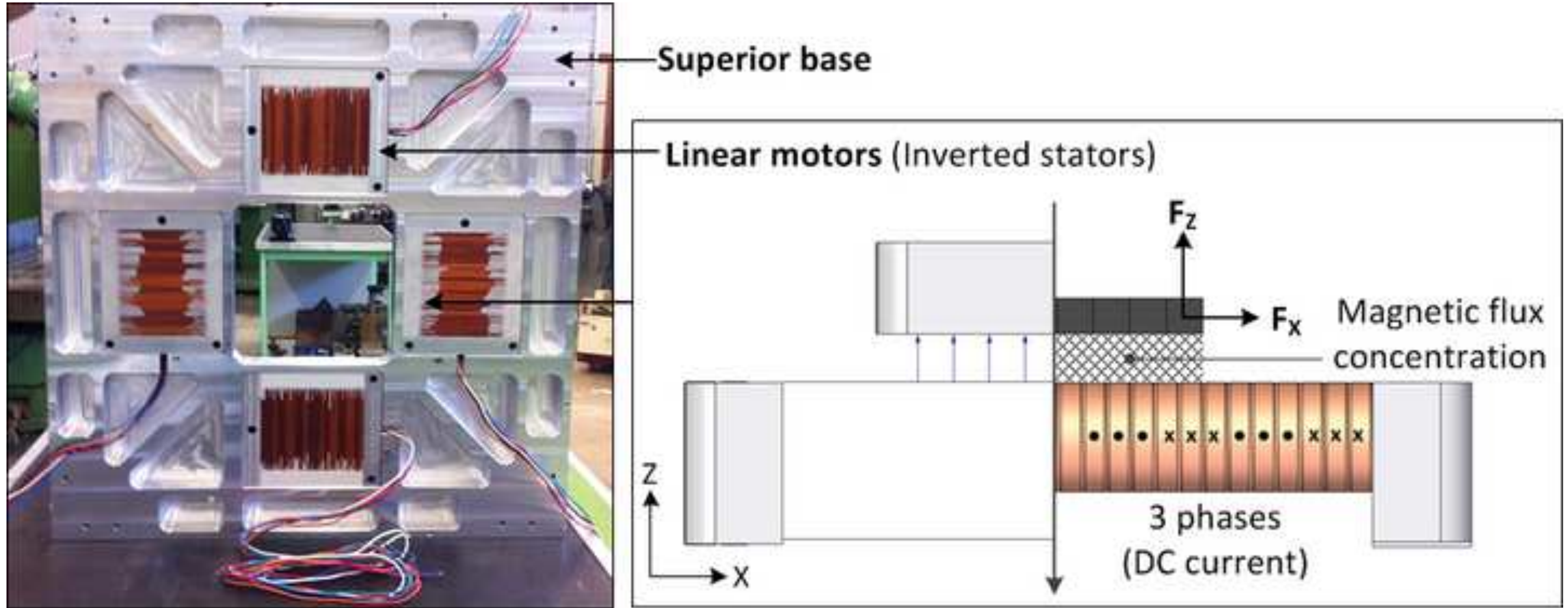

Figure8

Click here to download high resolution image

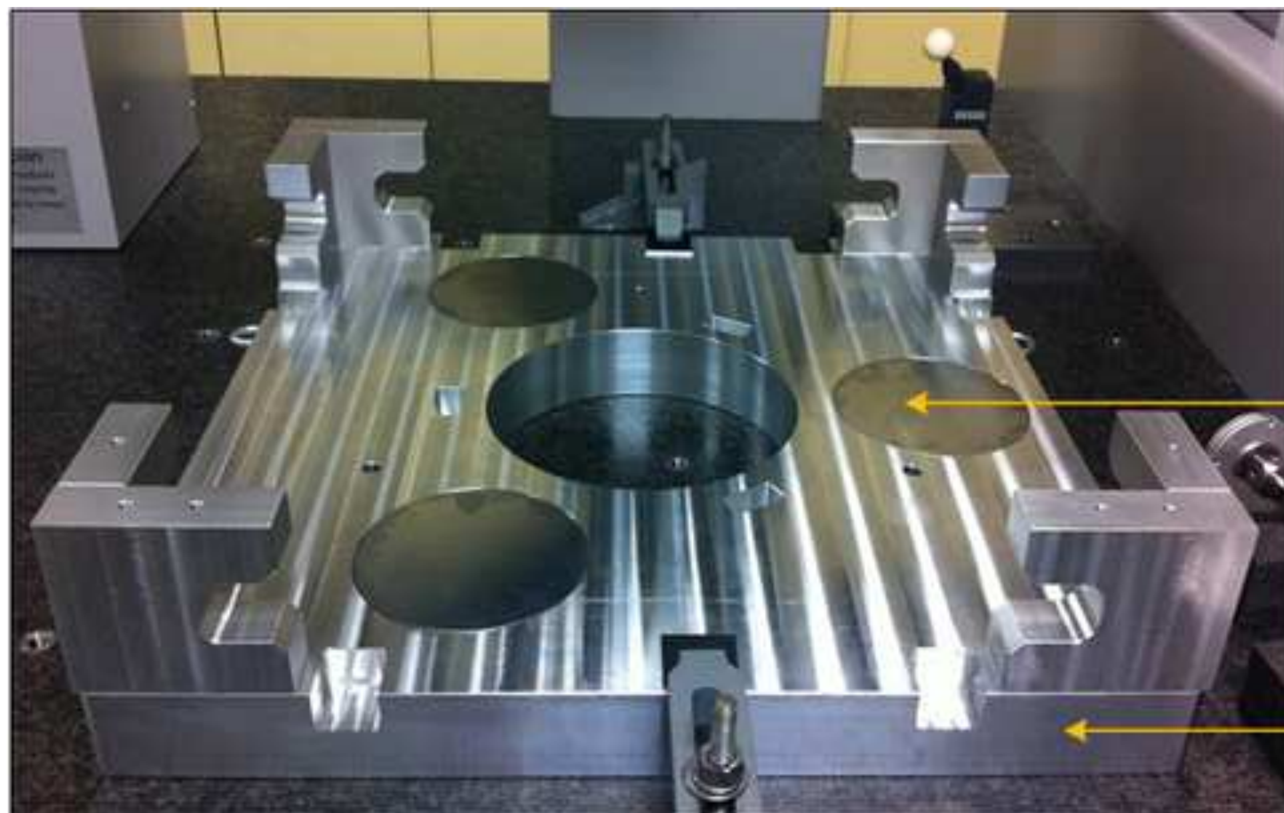

Vacuum preloaded air bearings
(Guide surfaces)

Inferior base structure
(Al 7075)

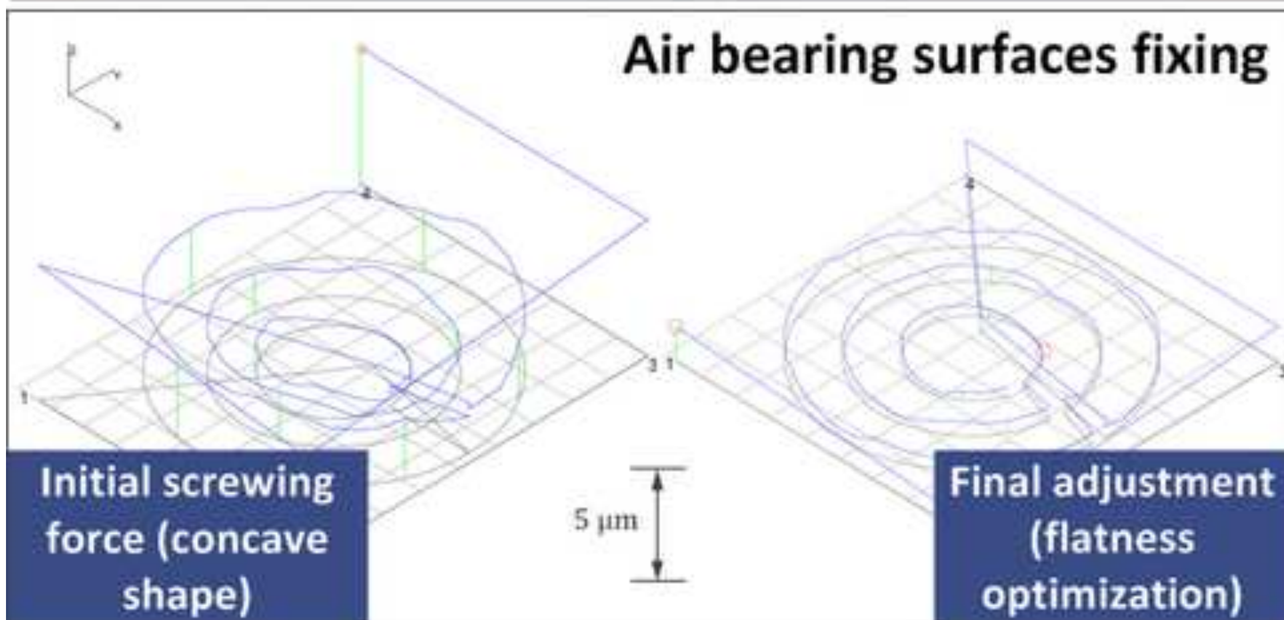

Figure9
Click here to download high resolution image

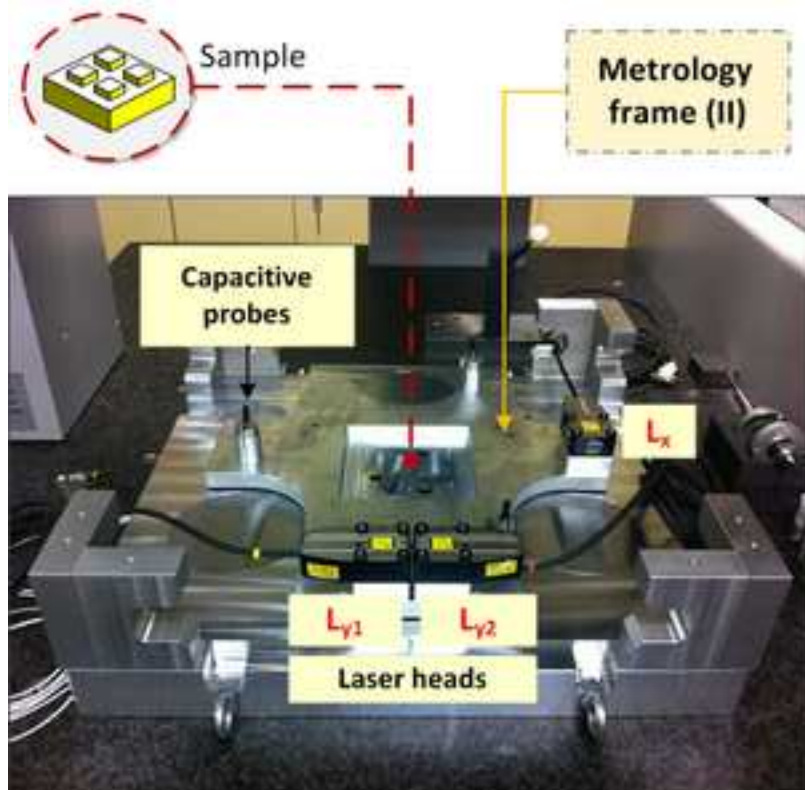

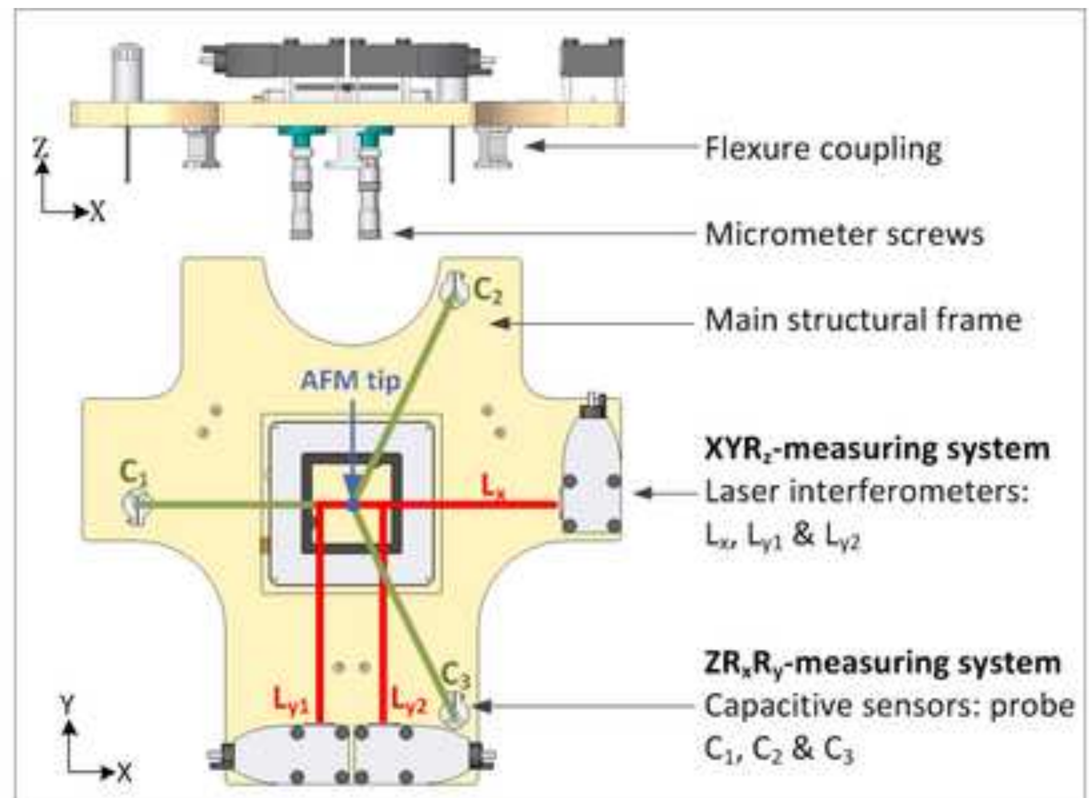

Figure10
Click here to download high resolution image

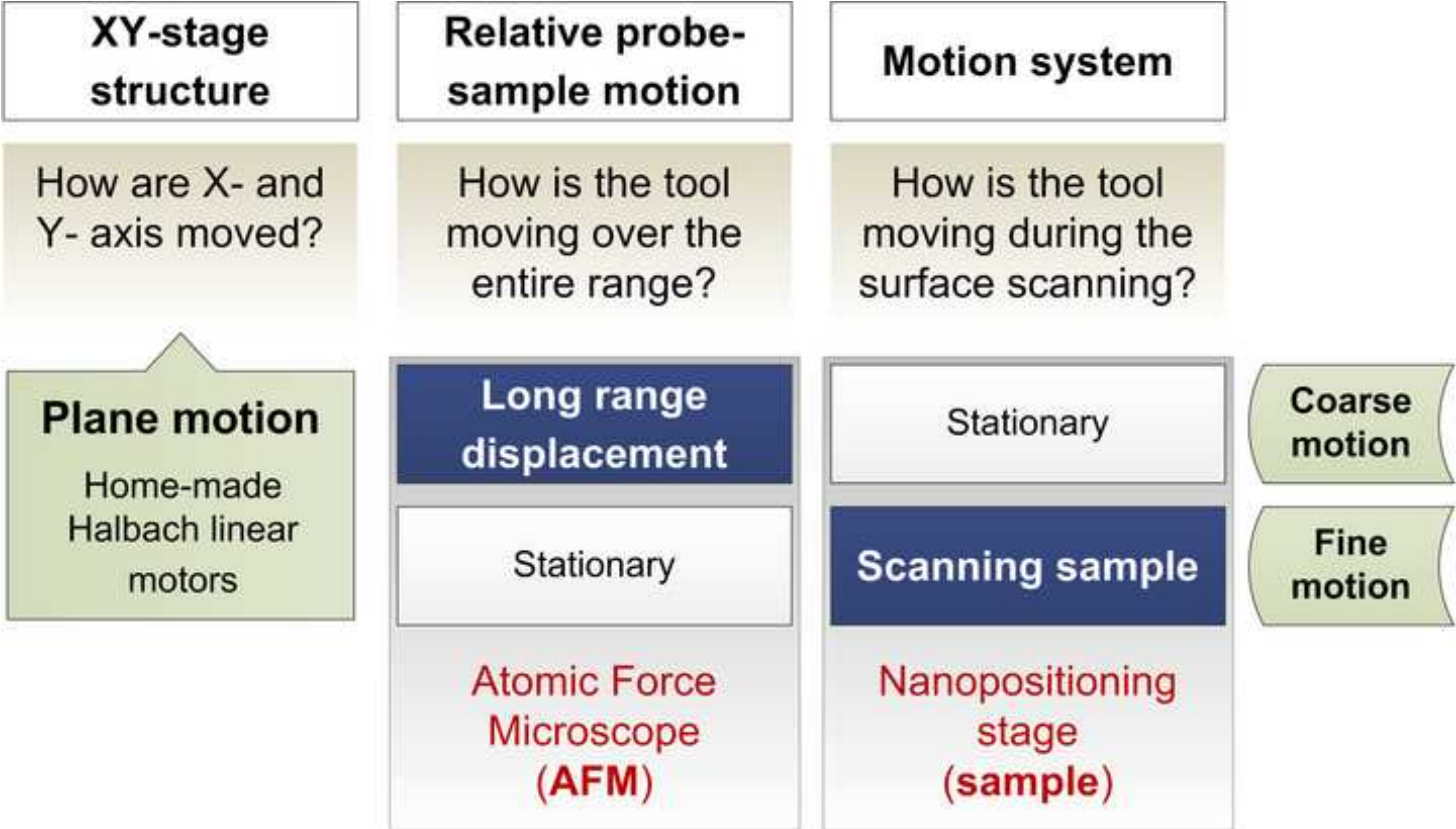

Figure11

Click here to download high resolution image

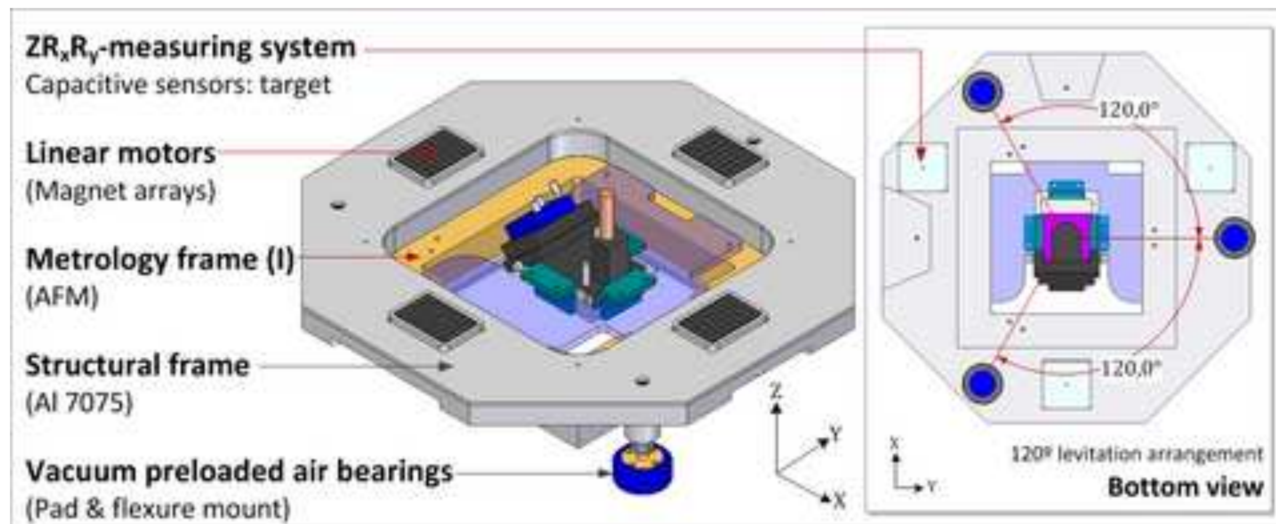

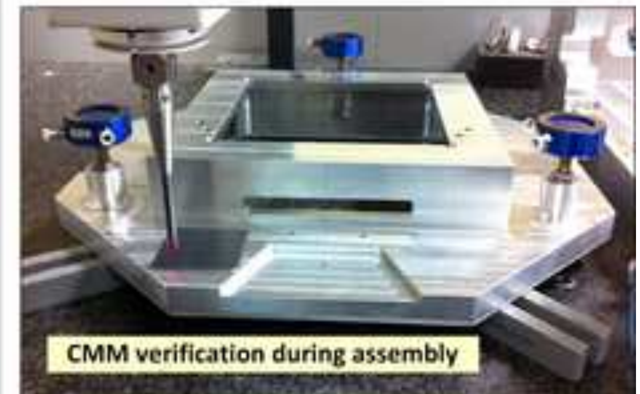

Figure12

Click here to download high resolution image